An Integrated Optimization Framework for Combined Heat and Power Units, Distributed Generation and Plug-In Electric Vehicles

Alireza Bostan[1], Mehrdad Setayesh Nazar[1], Miadreza Shafie-khah[2], and João P. S. Catalão[3,*]

[1] *Shahid Beheshti Univ., A.C., Tehran, Iran*
[2] *School of Technology and Innovations, University of Vaasa, 65200 Vaasa, Finland*
[3] *Faculty of Engineering of the University of Porto and INESC TEC, 4200-465 Porto, Portugal*
[*] *catalao@fe.up.pt*

Abstract

This paper provides a six-level integrated optimization framework for a distribution system that transacts energy with upward electricity market and downward active microgrids in day-ahead and real-time horizons. The proposed method uses a risk-averse formulation and the distribution system utilizes multiple combined heating and power units, distributed generation, plug-in electric vehicles parking lots, and electric and thermal storage units. Demand response program alternatives are also utilized by the distribution system. A three-stage uncertainty modeling is proposed to model six sources of uncertainties that are consist of energy resource power generations, loads and prices, active microgrids contributions and contingencies. Two case studies evaluate the proposed algorithm for the 123-bus test system that multiple 33-bus microgrid systems are transacting energy and ancillary services with the main grid. Further, different sensitivity analyses are performed to evaluate the effect of energy and ancillary services prices on the simulation results.

Keywords: Distributed Energy Resource; Active Distribution System; Microgrid; Demand Response; Bidding Strategy.

Nomenclature

Abbreviation

AC	Alternative Current.
ADS	Active Distribution System
ADSO	ADS Operator
AMG	Active Micro Grid.
ARIMA	Autoregressive Integrated Moving Average
CB	Capacitor Bank.
CHP	Combined Heating and Power.
CVaR	Conditional Value at Risk.
DA	Day-Ahead.
DER	Distributed Energy Resource.
DG	Distributed Generation.

DLC	Direct Load Control.
DRP	Demand Response Program.
DSO	Distribution System Operator
ESS	Electrical Storage System.
EV	Electric Vehicles
LMP	Locational marginal price
MG	MicroGrid.
MILP	Mix Integer Linear Programming.
MINLP	Mixed Integer Non-Linear Programming.
MMG	Multi-MicroGrid.
MUs	Monetary Units.
MMUs	Million MUs.
PGA	Parallel Genetic Algorithm.
PHEV	Plug-in Hybrid Electric Vehicle.
PL	Parking Lot
PVA	Solar Photovoltaic Array.
PU	Per-unit.
RL	Responsive Load.
RTP	Real Time Pricing.
RT	Real Time.
OBSADS	Optimal Bidding Strategy of ADS.
SW	Switching device.
SWT	Small Wind Turbine.
TES	Thermal Energy Storage.
TOU	Time Of Use
V2G	Vehicle to Grid.

Parameters

A	PVA area (m^2)
C_{CHP}	Operational costs of CHP unit (MUs).
C_{ESS}	Operational costs of electricity storage (MUs).
C_{TES}	Operational costs of thermal storage (MUs).
C_{DG}	Operational costs of DG (MUs).
C_{Boiler}	Operational costs of boiler (MUs).
$C_{Purchase}$	Cost of electricity purchased from upward utility (MUs).
C_{DRP}	Cost of demand response program (Mus).
C_{Op}	Operational cost (MUs/MWh).
C_{M}	Maintenance cost (MUs/MWh).

I	Solar irradiation of ADS PVA (kW/m).
ξ	ADS photovoltaic array conversion efficiency.
t_0	Outside air temperature (°C).
LMP	Locational marginal price (MU/MW).
$NAMGS$	Number of AMGs.
$NOIS$	Total number of ADS scenarios.
$NDAS$	Total number of DA energy, spinning reserve and reactive market scenarios.
$NOSS$	Total number loads and PHEV contributions and DER generation scenarios.
$NCSS$	Total number of contingency scenarios.
P^{Load}	Electric power of electrical load (kW).
P^{PVA}	Electric power generated by photovoltaic array (kW).
P^{ESS}	Electric power delivered by electricity storage (kW).
$P_{Critical}^{Load}$	Critical electrical load (kW).
$P_{Controllable}^{Load}$	Controllable electrical load (kW).
P^{SWT}	Electric power generated by SWT.
ΔP^{DLC}	Electric power withdrawal changed for DLC program (kW).
$Penalty$	Penalty of active or reactive power mismatch that paid to upward market (MU)
$prob$	Probability of contingency.
ϖ_{PHEV}^{Charge}	Charge limitation ratio.
$\varpi_{PHEV}^{Discharge}$	Discharge limitation ratio.
$\kappa_{Purchased}^{Elect}$	AMG electricity purchasing price that is purchased from ADS (MUs/kWh).
κ_{DLC}^{Elect}	Price of DLC program implementation (MUs/kWh).
κ_{TOU}^{Elect}	Price of TOU program implementation (MUs/kWh).
κ_{Sell}^{Elect}	AMG electricity selling price that is sold to ADS (MUs/kWh).
T	Total operation time of facility (Hour).

Variables

$ENPHEV$	State of charge of PHEV.
W	Weight factor.
α	Confidence level.
β	Weighting parameter for risk-aversion attitude.
γ	Probability of contingency.
ψ	Binary decision variable of device operation (equals to 1 if device operates).
τ	Duration of device operation.
μ, ζ	Auxiliary variable used to compute the CVaR.
λ^{active}	Active power price sold to the upward market (MUs/kW).
λ^{SR}	Spinning reserve price sold to the upward market (MUs/kW).

$\lambda^{reactive}$	Reactive power price sold to the upward market (MUs/kVAr).
$P_{DA\_upward}^{active}$	Active power sold to the upward DA market (kW).
SR_{DA_upward}	Spinning reserve sold to the upward DA market (kW).
$Q_{DA\_upward}^{reactive}$	Reactive power sold to the upward DA market (kVAr).
$\eta_{DA\_downward}^{active}$	Active power price sold to the downward loads (MUs/kW).
$\eta_{DA\_downward}^{reactive}$	Reactive power price sold to the downward loads (MUs/kVAr).
$P_{DA\_downward}^{active}$	Active power sold to the downward loads (MUs/kW).
$Q_{DA\_downward}^{reactive}$	Reactive power sold to the downward loads (MUs/kVAr).
P	Active power (kW).
Q	Reactive power (kVAr).
Q'^{Load}_{AMG}	Thermal load of AMG (kW_{th}).
Q'^{B}_{AMG}	Boiler thermal power output of AMG (kW_{th}).
Q'^{Loss}	Loss of thermal power (kW_{th}).
Q^{Loss}	Reactive power loss (kVAr).
Q_{AMG}^{DRP}	DRP reactive power of AMG (kVAr).
Q_{AMG}^{Load}	Load reactive power of AMG (kVAr).
ΔP^{TOU}	Change in load based on TOU program (kW).
P_{Shed}	Shed load (kW).
V	Voltage of ADS bus (kV).
δ	Voltage angle of ADS bus (rad).
v_c^{Wind}	Small wind turbine cut-in wind velocity.
v_f^{Wind}	Small wind turbine cut-off wind speed.
T_{Boiler}	Aggregated duration of compression chiller operation.
T_{ESS}	Aggregated duration of ESS operation.
T_{CHP}	Aggregated duration of CHP operation.
T_{TES}	Aggregated duration of TES operation.

1. Introduction

The Active Distribution Systems (ADSs) can transact electrical energy with the downward Active MicroGrids (AMGs) [1] and custom loads and/or its upward electricity market [2], as shown in Fig. 1. The ADS can participate in the upward wholesale market and optimize its bid in upward wholesale energy, spinning reserve and reactive power markets. In addition, some of the AMGs can purchase active and reactive power from the ADS; meanwhile, other AMGs can sell active power and reactive power to it [3].

The ADS can use different Demand Response Programs (DRPs) alternatives to encourage AMGs to optimize and coordinate their bids. The AMGs contribution scenarios can be optimized and the optimal coordinated scheduling of ADS and AMGs can be determined. Thus, a non-equilibrium model can be extended and in the proposed model the Day-Ahead (DA) joint energy, spinning reserve and reactive power markets bidding strategy of ADS. Further, the updated system data can be utilized for joint energy and reactive power Real-Time (RT) markets and the optimization procedure can be performed [4].

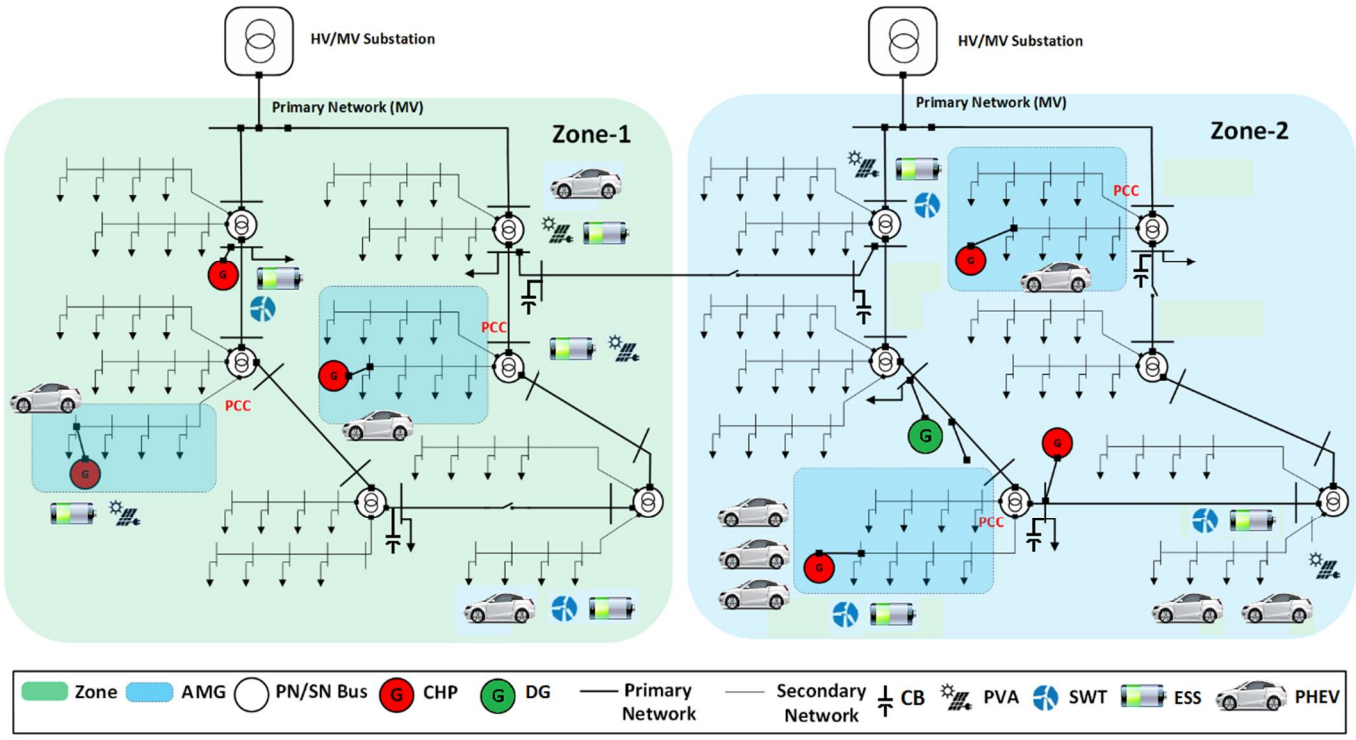

Fig. 1. Representation of ADS with its downward AMGs.

The Optimal Bidding Strategy of ADS (OBSADS) problem consists of DA and RT scheduling of the system distributed energy resources considering of the downward AMGs bidding strategies, system contingencies and stochastic behavior of different sources of uncertainties [4].

As shown in Table 1 and based on its categorization, different aspects of the optimal bidding strategy problem have been studied over the recent years and the literature can be categorized into the following groups.

The first category presents the optimal scheduling of the downward MicroGrids (MGs) and/or Parking Lots (PLs) energy resources that transact electricity with the upward distribution system [5-25]. These researches only models and dispatches the MG/PLs facilities to minimize the operational costs and/or maximize the revenue of the facilities owner. The second category proposes optimal scheduling of ADS that considers the downwards MGs/PLs as ADS dispatchable energy resources. These papers do not model the ADS and MGs/PLs interactions [26-28]. The third category simultaneously models the optimal scheduling of energy resources of ADS and MGs/PLs and considers the interactions of the ADS and the downwards MGs [29-31].

Based on the above categorization and for the first category of researches, Ref. [5] presents a cost minimization model of MGs to schedule dispatchable DERs that uses robust optimization algorithm and the research concludes that the integration of Combined Heat and Powers (CHPs) helps to decrease system spending. Ref. [6] presents a two-stage algorithm for the scheduling of Vehicle to Grids (V2Gs) and Responsive Loads (RLs) to minimize emissions and costs considering of DERs. In the first stage, the power generation costs are minimized; meanwhile, in the second stage, the costs of DERs' power generation deviations are minimized.

Ref. [7] introduces a two-stage daily scheduling strategy for DERs located in a distribution system with a substantial Solar Photovoltaic Array (PVA) penetration. At the first stage, a portion of the DERs capacity is dispatched for regulation, while the remaining capacity is considered for energy exchange and minimising the deviations from the forecast. Ref. [8] proposes a two-stage stochastic optimization model for the DA energy and secondary reserve markets. The objective function is proposed as cost minimization of transactions in DA and RT markets. The proposed bidding strategy reduces the costs by 40% compared to retailers' bidding strategy.

Ref. [9] presents an optimal stochastic metaheuristic scheduling algorithm for the networked microgrids considering uncertainties of DERs and time of use (TOU) and real-time pricing (RTP) programs. Ref. [10], explores the day-ahead scheduling of CHP systems considering Thermal Energy Storage systems (TESs), DERs and boilers based on an Autoregressive Integrated Moving Average (ARIMA) algorithm for generating of the demand and electricity price

scenarios. Ref. [11] presents a heuristic optimization model for optimal day-ahead operational planning that minimizes pollutant emission and operating cost and the approach also considers energy storage systems. Ref. [12], proposes a scheduling algorithm that uses information gap method to model the wholesale electricity market uncertainties. The critical profit method is implemented for risk-averse units through the robust optimization algorithm to ensure that the future electricity prices fall into a maximized robustness region.

Ref. [13] presents a bi-level algorithm to optimize interactions between distribution system operator and PL agent that the upper-level problem minimizes the cost of Distribution System Operator (DSO); meanwhile, the lower-level problem schedules the energy and reserve of the parking lot owner.

Ref. [14] presents the optimal bidding strategy of a microgrid in the joint energy and ancillary service markets using hybrid stochastic/robust optimization. The proposed method increases the microgrid revenues by 24.75% with respect to the base case that microgrid only bids in the energy market.

Ref. [15] introduces a two-stage stochastic algorithm to minimize the reserve cost that is used for compensating the intermittent DER power generation forecast errors. The model considers RLs and gas-fired Distributed Generations (DGs). Ref. [16], presents an algorithm for maximizing of CHP-based AMG considering Small Wind Turbine (SWT) power generation and wholesale market uncertainties.

Ref. [17] a two-stage Mixed-Integer Linear Programming (MILP) stochastic optimization algorithm is proposed to minimize the operation cost. Ref. [18] proposes an algorithm for stochastic energy and reserve scheduling that uses DRPs in either energy or reserve schedule. The results show that the DRP can reduce operating costs. Ref. [19] presents a model for Electrical Storage System (ESS) that is used to optimize energy exchange and to balance out the uncertain electrical vehicles loads. The results show the viability of the proposed method of providing cost savings. Ref. [20] presents the optimal operation framework for the Multi MicroGrids (MMGs). A two-stage robust optimization is used to minimize the operating cost under the worst case of PVAs outputs. The results show that the algorithm reduces the operating cost; meanwhile, mitigates the energy interaction between the MMG and the upward grid. Ref. [21] presents a multi-objective scheduling algorithm for Electric Vehicles (EVs) that minimizes operational costs and emissions. The Benders decomposition technique is used to solve the optimization model and the proposed method is tested on a 33-bus system. Ref. [22] the optimal operation of a distribution system is evaluated considering DERs, DRPs and EVs. The proposed model is tested on the IEEE 15-bus distribution system.

The first category of researches did not consider contingencies, ADS optimization procedure and decision variables, heating loads and topology optimization of MGs and ADS.

The second category only considers the scheduling problem of ADS without the detailed model of the downwards MGs/PLs. Ref. [23] proposes an estimation method to minimize the operating costs and increasing reliability of the system that uses a meta-heuristic optimization algorithm. The algorithm considers DRPs associated with reconfiguration of system. Ref. [24] introduces the application of microgrids in mitigating the load variability. The algorithm utilizes the microgrid scheduling procedure to coordinate the net load of the upward distribution network considering the constraints of microgrids.

Ref. [25] presents bi-level optimization algorithm for scheduling of ADS that in the first level the system resources are allocated to minimize system loss, meanwhile; in the second level, hourly energy and ancillary service generation of DERs are optimized. Ref. [26] introduces risk-based optimal scheduling of reconfigurable system that maximizes profit the distribution system operator. Ref. [27] proposes a two-level algorithm for scheduling of distribution networks with multi-microgrids. The upper-level problem considers the distribution system constraints and optimizes the transaction price; meanwhile, the lower-level problem minimizes the operation cost. The interaction of upper and lower problem is formulated as a Stackelberg game. Ref. [28] presents a stochastic optimization model to minimize the operational cost and reliability cost. The bat optimization algorithm is used to solve the problem and the uncertainties of SWTs, PVAs and the EVs are considered.

The introduced second category of researches did not consider contingencies, MGs optimization procedure, RT market, security constraints, heating loads and topology optimization of MGs and ADS.

The third category considers the ADS and MGs/PLs interactions and optimization procedures. Ref. [29] introduces a recursive two-level optimization framework to model the interactions between the distribution system and energy hubs.

Ref. [30] proposes the home microgrids optimal operation and considers the microgrid interoperability with distribution system. A non-cooperative gaming formulation is utilized to model the optimal coordination of ADS and MGs strategies and DRP alternatives are modeled. Ref. [31] introduces the DRP aggregator bidding strategy and considers the distribution system operator decision variables using game theory. The robust optimization is utilized to model the price uncertainties. The introduced third category of researches did not consider contingencies, RT market, security constraints, heating loads and topology optimization of MGs and ADS.

Based on the above categorization, an integrated framework that considers the optimal bidding of ADS in the DA and RT joint electricity markets and simultaneously models the ADS and AMGs interactions in normal and contingent conditions is less frequent in the literature.

Table 1 provides the comparison between the proposed OBSADS model with other approaches.

Accordingly, the novel contributions of this paper are:

- A six-level Mixed-Integer Non-Linear Programming (MINLP) algorithm takes into account power transactions between downward AMGs and ADS,
- A stochastic algorithm models six sources of uncertainty:
  i. The upward day-ahead market energy, spinning reserve and reactive power services prices,
  ii. The day-ahead heating and electrical loads, and AMGs loads,
  iii. Charge and discharge of PHEVs,
  iv. The DERs and AMGs electricity generation,
  v. The upward RT market energy, spinning reserve and reactive power services price,
  vi. The ADS electrical system contingencies.
- A framework concurrently optimizes the ADS and AMGs objective functions and ponders the optimal coordination of ADS resources in the contingent condition.

Table 1: Comparison of the proposed approach with other studies.

References		5	6	7	8	9	10	11	12	13	14	15	16	17	18	19	20	21	22	23	24	25	26	27	28	29	30	31	Proposed Approach
Method	MILP	✓	×	✓	×	×	✓	×	×	✓	✓	×	✓	✓	✓	×	×	×	×	×	✓	×	×	×	×	✓	×	×	×
	MINLP	×	×	×	×	×	×	×	✓	×	×	×	×	×	✓	×	×	✓	×	×	×	×	✓	×	×	×	×	×	×
	Heuristic	×	✓	×	✓	✓	×	✓	×	×	×	✓	×	×	×	×	✓	×	✓	✓	×	✓	✓	✓	✓	×	✓	✓	✓
Model	Deterministic	×	×	×	×	✓	✓	✓	×	✓	×	×	×	×	×	×	×	✓	×	✓	✓	✓	×	×	×	×	✓	×	×
	Stochastic	✓	✓	✓	✓	×	×	×	✓	×	✓	✓	✓	✓	✓	✓	✓	×	✓	×	×	×	×	✓	✓	✓	×	✓	✓
Objective Function	Revenue	×	×	×	✓	×	×	×	✓	×	✓	×	×	×	×	×	×	×	✓	×	×	×	✓	×	×	×	×	×	✓
	Gen. Cost	✓	✓	×	✓	✓	×	✓	✓	✓	✓	✓	×	✓	✓	×	×	✓	✓	✓	✓	✓	✓	✓	✓	×	✓	✓	✓
	ESS Cost	×	×	✓	✓	✓	×	✓	×	×	✓	×	×	✓	×	✓	✓	×	×	✓	×	×	×	✓	×	×	×	×	✓
	Security Costs	×	✓	×	×	×	×	×	×	×	×	×	×	×	✓	×	×	×	×	×	✓	×	×	×	✓	×	×	×	✓
	PHEV	×	✓	×	×	×	×	×	×	✓	×	×	×	×	×	✓	✓	✓	×	×	×	×	×	×	✓	×	×	×	✓
	DRP	×	✓	×	×	✓	✓	×	×	×	×	✓	✓	✓	✓	×	×	×	✓	✓	×	×	×	✓	×	×	×	✓	✓
	SWT	×	✓	×	×	×	×	×	×	×	✓	✓	✓	✓	✓	×	×	×	×	✓	×	✓	✓	×	✓	×	×	×	✓
	PVA	×	✓	✓	✓	×	×	×	×	×	✓	✓	×	✓	✓	×	✓	×	×	✓	×	×	×	×	✓	×	×	×	✓
CHP Nonlinearity		×	×	×	×	×	✓	×	✓	×	×	×	✓	✓	×	×	×	×	×	×	×	×	×	×	×	×	×	×	✓
Single or Bi-level	DSO optimization	×	×	×	×	×	×	×	×	×	×	×	×	×	×	×	×	×	×	×	×	×	✓	✓	✓	✓	✓	✓	✓
	MG optimization	✓	✓	✓	✓	✓	✓	✓	✓	✓	✓	✓	✓	✓	✓	✓	✓	✓	✓	✓	✓	✓	×	×	×	✓	✓	✓	✓
DA-Market		✓	✓	✓	✓	✓	✓	✓	✓	✓	✓	✓	✓	✓	✓	✓	✓	✓	✓	✓	×	✓	✓	✓	✓	×	×	×	✓
RT- Market		×	×	✓	✓	×	×	×	×	×	×	×	×	×	×	×	×	×	×	×	×	×	×	×	×	×	×	×	✓
OBSADS		×	×	✓	×	×	×	×	×	×	×	×	×	×	×	✓	×	×	×	×	×	×	×	×	×	×	×	×	✓
Uncertainty Model	PHEV	×	✓	×	×	×	×	×	×	×	×	×	×	×	×	✓	✓	×	×	×	×	×	×	×	✓	×	×	×	✓
	DERs	×	✓	✓	×	×	×	×	×	✓	✓	×	×	✓	✓	×	✓	×	✓	✓	×	✓	✓	×	✓	×	×	×	✓
	DA Market	✓	×	✓	✓	×	✓	×	×	×	✓	×	✓	×	×	×	×	×	×	×	×	×	×	×	×	×	×	×	×	✓
	RT Market	×	×	✓	✓	×	×	×	×	×	×	×	×	×	×	×	×	×	×	×	×	×	×	×	×	×	×	×	×	✓
	Contingency	×	×	×	×	×	×	×	×	×	×	×	×	×	×	×	×	×	×	×	×	×	×	×	×	×	×	×	×	✓
	Loads	×	✓	✓	✓	×	✓	×	×	✓	×	×	✓	✓	×	✓	×	×	×	×	×	✓	×	×	×	×	×	×	×	✓
Storage System	EES	×	×	✓	✓	✓	✓	✓	×	×	✓	×	✓	×	✓	✓	✓	×	✓	✓	×	×	×	✓	✓	✓	✓	×	✓
	TES	×	×	×	×	×	✓	×	×	×	×	×	✓	✓	×	×	×	×	×	×	×	×	×	×	×	×	×	×	×	✓
AC model		×	×	×	×	×	×	✓	×	×	×	×	×	×	✓	×	×	✓	✓	✓	×	×	✓	✓	✓	✓	×	×	✓
Reconfiguration		×	×	×	×	×	×	×	×	×	×	×	×	×	×	×	×	×	×	✓	×	×	✓	×	×	×	×	×	✓
Category		1	1	1	1	1	1	1	1	1	1	1	1	1	1	1	1	1	1	1	1	1	2	2	2	3	3	3	3

2. Problem Modeling and Formulation

As shown in Fig.2, the ADS Operator (ADSO) utilizes CHP systems to supply its heating and electrical loads and downward AMGs. ADS is equipped with the gas-fired DG and boilers, PVAs, SWTs, ESSs, and TESs, PHEV parking lots, and RLs. The ADSO can vend its electricity excess to the upward wholesale market; meanwhile, AMGs can sell their electricity to the ADS. The ADS transacts energy with its DERs and AMGs and upward electricity market; meanwhile, it purchases spinning reserve from AMGs, PHEV parking lots, ESSs and DGs.

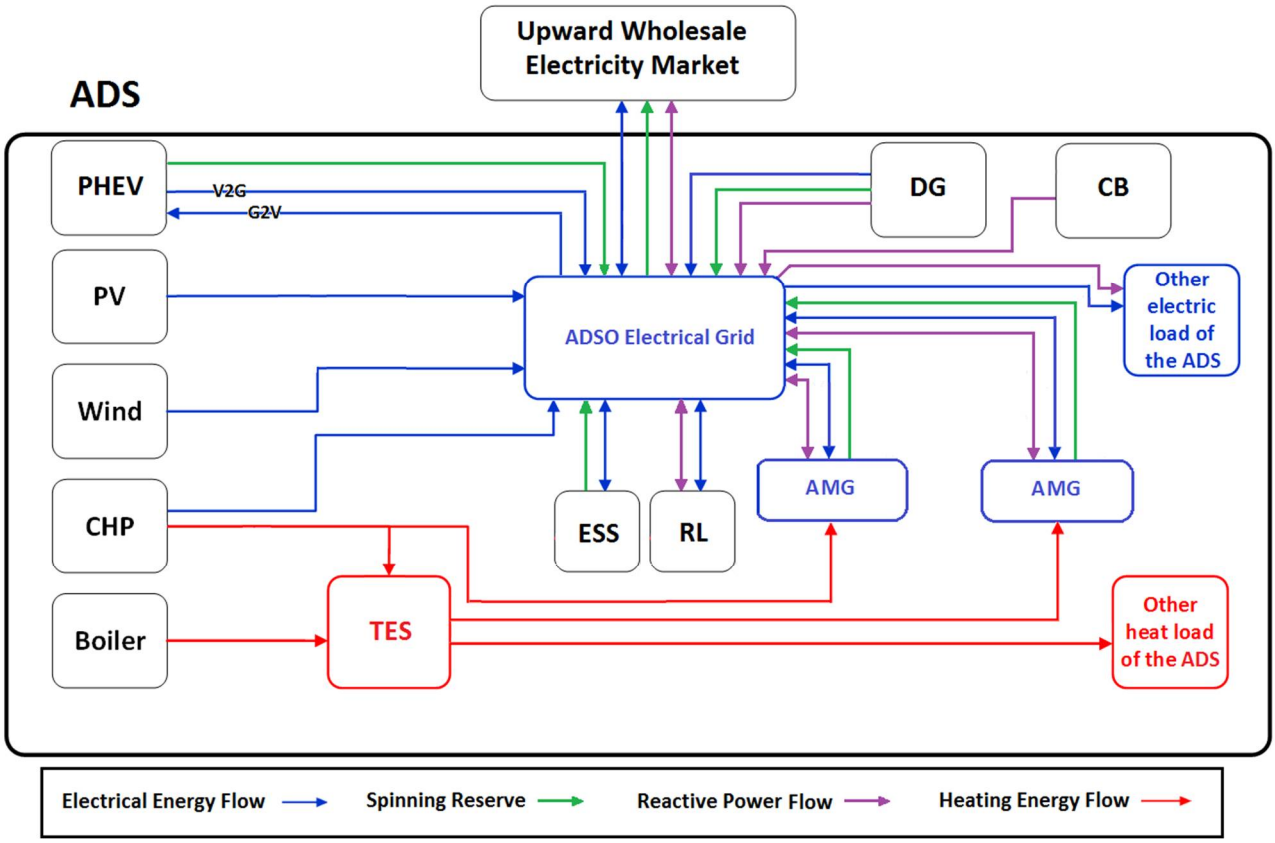

Fig. 2. ADSO energy resources and transactions.

The OBSADS must maximize the ADSO and AMGs revenues and the reliability of provided services for the downward heating and electrical loads [28]. The OBSADS must optimize joint energy, spinning reserve and reactive power selling/purchasing based on the fact that this procedure may provide a higher profit for the ADS than selling energy alone as a commodity [32]. The described OBSADS problem has different sources of uncertainties.

2.1. Uncertainty modeling

The OBSADS problem is subject to the six sources of uncertainty: 1) the upward day-ahead market energy, spinning reserve and reactive power services prices; 2) The day-ahead heating and electrical loads, and AMGs loads, 3) Charge and discharge of PHEVs; 4) the DERs and AMGs electricity generation; 5) the upward RT market energy and reactive power services price; 6) and the ADS's electrical system contingencies.

As shown in Fig.3, a multi-level optimization algorithm is proposed that the ADSO must make optimal decisions throughout OBSADS horizon with incomplete information and it determines the optimal values of problem decision variables.

In the day-ahead market, the ADSO uses an estimated data of the upward wholesale electricity market price, hourly electrical and heating loads, and hourly DERs power generation to determine optimal generation schedules of its energy generation units, electricity transactions with wholesale market and AMGs, estimated DRPs control variables and contingency-based load shedding alternatives.

At the first stage of uncertainty modeling, the ADSO estimates the upward day-ahead market energy, spinning reserve and reactive power services prices. At the second stage of uncertainty modeling, the ADSO estimates the DERs and AMGs electricity generation, the hourly heating and electrical loads consist of charge and discharge of PHEVs. Further, the AMGs' bid/offer scenarios are explored by the OBSADS that is explained in the following section. Then, the day-ahead optimal scheduling of ADS energy resources are determined and the accepted AMGs' bid/offer are determined. Finally, at the third stage of uncertainty modeling, contingency scenarios are generated and the OBSADS determines the involuntary load shedding, corrective DRPs and accepted AMGs' bid/offer values for each contingency scenario and the ADS system resources are re-dispatched.

The accepted spinning reserve bids in the DA market must be controlled as fixed parameters in the RT markets and any deviation of spinning reserve parameters are penalized by the upward market operator.

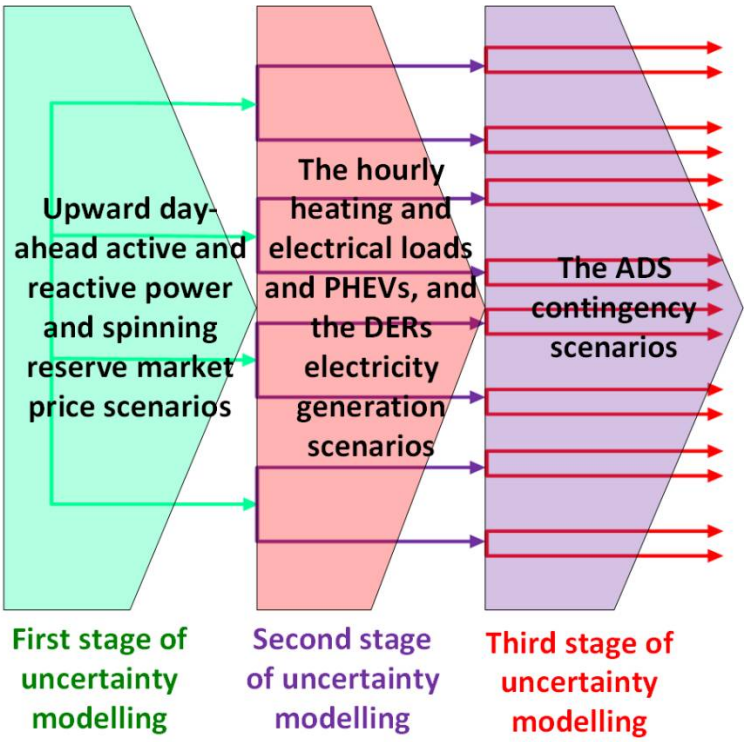

Fig. 3. The uncertainty modeling of the OBSADS problem.

2.2. ADS DA Optimization Problem Formulation

A six-level optimization algorithm is presented for the proposed model. The first level objective function of OBSADS is given in (1) for the DA joint energy, spinning reserve and reactive power markets. The NOIS parameter is the total number of ADS normal and contingency-based scenarios.

$$Max\ \mathsf{M}_1 = \sum_{NOIS} prob.\left(\begin{array}{l} W_1(revenue_{ADS} - \{(C_{ADS}^{CHP}.\psi_{ADS}^{CHP} + C_{ADS}^{ESS}.\psi_{ADS}^{ESS} + C_{ADS}^{TES}.\psi_{ADS}^{TES} + C_{ADS}^{DG}.\psi_{ADS}^{DG} \\ + C_{ADS}^{Boiler}.\psi_{ADS}^{Boiler}) + C_{ADS}^{Purchase} + C_{DRP}^{AMG} + \sum Penalty^{active} + \\ \sum Penalty^{reactive}) - W_2(\sum_{NL} LMP.P_L - \sum_{NG} LMP.P_G) \end{array}\right) \quad (1)$$

$$+\beta(\zeta - \frac{1}{1-\alpha}\sum_{NOIS} prob.\mu)$$

The objective function is divided into seven groups: 1) the revenue of ADS($revenue_{ADS}$); 2) the commitment costs of ADS' DERs consist of CHP, ESS, TES, DG, and boiler $(C_{ADS}^{CHP}.\psi_{ADS}^{CHP} + C_{ADS}^{ESS}.\psi_{ADS}^{ESS} + C_{ADS}^{TES}.\psi_{ADS}^{TES} + C_{ADS}^{DG}.\psi_{ADS}^{DG} + C_{ADS}^{Boiler}.\psi_{ADS}^{Boiler})$ that the ψ variable is the binary decision variable of device operation; 3) the energy purchased from wholesale market costs ($C_{ADS}^{Purchase}$); 4) the costs of AMGs' DRPs

(C_{DRP}^{AMG}); 5) the penalties of deviations in active and reactive markets ($\sum Penalty^{active} + \sum Penalty^{reactive}$); 6) the difference of Locational Marginal Price (LMP) of load and generation buses ($\sum_{NL} LMP.P_L - \sum_{NG} LMP.P_G$); and 7) the $CVaR$ is minimised that is defined at the α confidence level ($CVaR_\alpha$) to control the risk ($\beta(\zeta - \frac{1}{1-\alpha}\sum_{NOIS} prob.\mu)$.

The LMP term is used to mitigate the energy price difference between zones of the distribution system for normal and contingent conditions. A risk-neutral attitude corresponds to $\beta = 0$, while a risk-averse attitude would correspond to $\beta > 0$ [26].

The revenue of ADS can be written as (2):

$$revenue_{ADS} = \begin{pmatrix} \sum \lambda^{active}.P_{DA\_upward}^{active} + \sum \lambda^{SR}.SR_{DA\_upward} + \sum \lambda^{reactive}.Q_{DA\_upward}^{reactive} + \\ \sum \eta_{DA\_downward}^{active}.P_{DA\_downward}^{active} + \sum \eta_{DA\_downward}^{reactive}.Q_{DA\_downward}^{reactive} \end{pmatrix} \quad (2)$$

Eq. (2) is divided into five groups: 1) the revenue of active power sold to the DA upward market ($\sum \lambda^{active}.P_{DA\_upward}^{active}$); 2) the revenue of spinning reserve sold to the DA upward market ($\sum \lambda^{SR}.SR_{DA\_upward}$); 3) the revenue of reactive power sold to the DA upward market ($\sum \lambda^{reactive}.Q_{DA\_upward}^{reactive}$); 4) the revenue of active power sold to the downward customers in the DA market ($\sum \eta_{DA\_downward}^{active}.P_{DA\_downward}^{active}$); and 5) the revenue of reactive power sold to the downward customers in the DA market ($\sum \eta_{DA\_downward}^{reactive}.Q_{DA\_downward}^{reactive}$).

If the ADS power factor is less than 0.95, then ADS will be penalized an additional fee. The power factor penalty is modelled as Eq. (3):

$$Penalty = k.Q^{\text{Reactive}} \quad \text{if } |\cos\varphi_{ADS}| \le \cos\varphi_{ADS}^{\min} \quad \text{else } =0 \quad (3)$$

$$\cos\varphi_{ADS} = \frac{P_{DA\_upward}^{active} + SR_{DA\_upward}^{Spinning}}{\sqrt{(P_{DA\_upward}^{active} + SR_{DA\_upward}^{Spinning})^2 + Q_{DA\_upward}^{active\ 2}}} \quad (4)$$

The k parameter is the penalty coefficient. The $P_{DA\_upward}^{active}$, $Q_{DA\_upward}^{active}$ and $SR_{DA\_upward}^{Spinning}$ parameters are the ADS bidding quantity to the upward wholesale energy, reactive power and spinning reserve, respectively.

The cost components of Eq. (1) are defined as the following equations:

$$C_X = \sum_{NOSS} prob.\sum_{T_X} \tau.(C_{Op}^X + C_M^X) \quad X \in \{CHP, DG\} \quad (5)$$

$$C_{Boiler} = \sum_{NOSS} prob.\sum_{T_{Boiler}} \tau.(C_{Op}^{Boiler} + C_M^{Boiler}) \quad (6)$$

$$C_Y = \sum_{NOSS} prob.\sum_{T_Y} \tau.(C_{Op}^Y + C_M^Y) \quad Y \in \{ESS, TES\} \quad (7)$$

Eq. (5) presents the expected commitment costs of CHPs and DGS that consist of operational and environmental costs for the aggregated duration of CHPs and DGs operation ($\sum_{T_x} \tau.(C_{Op} + C_M)$). Eq. (5) considers the total number of loads and PHEV contributions and DER generation scenarios in *NOSS* parameters.

Eq. (6) considers the expected commitment costs of boilers that is decomposed into operational and environmental costs of boiler ($\sum_{T_{Boiler}} \tau.(C_{Op}^{Boiler} + C_{M}^{Boiler})$). Further, Eq. (7) introduces the commitment costs of ESSs and TESs ($\sum_{T_Y} \tau.(C_{Op}^{Y} + C_{M}^{Y})$).

Electric power balance constraint of ADS is given as (8):

$$\sum P_{ADS}^{CHP} + \sum P_{ADS}^{DG} \mp \sum P_{ADS}^{AMG} - \sum P_{ADS}^{Loss} - \sum P_{ADS}^{Load} \mp \sum P_{ADS}^{ESS} \mp \sum P_{ADS}^{PHEV} + \sum P_{ADS}^{SWT} + \sum P_{ADS}^{PVA} \mp \sum P_{ADS}^{DRP} = 0 \quad (8)$$

Eq. (8) terms are the CHPs and DGs active power generation ($\sum P_{ADS}^{CHP} + \sum P_{ADS}^{DG}$), the AMGs active power withdrawal/injection from/to the ADS ($\mp \sum P_{ADS}^{AMG}$), active power loss ($\sum P_{ADS}^{Loss}$),active power withdrawal of load ($-\sum P_{ADS}^{Load}$), the ESSs active power withdrawal/injection from/to the ADS ($\mp \sum P_{ADS}^{ESS}$), the PHEVs active power withdrawal/injection from/to the ADS ($\mp \sum P_{ADS}^{PHEV}$), the SWTs and PVAs active power generation ($\sum P_{ADS}^{SWT} + \sum P_{ADS}^{PVA}$), and the DRPs active power withdrawal/injection from/to the ADS ($\mp \sum P_{ADS}^{DRP}$) for each interval of simulation.

The heating power balance constraint can be written as (9):

$$\sum Q_{ADS}^{CHP} + \sum Q_{ADS}^{DG} + \sum Q_{ADS}^{AMG} - \sum Q_{ADS}^{Loss} \pm \sum Q_{ADS}^{DRP} = 0 \quad (9)$$

Eq. (9) terms are the CHPs and DGs reactive power generation ($\sum Q_{ADS}^{CHP} + \sum Q_{ADS}^{DG}$), the AMGs reactive power withdrawal/injection from/to the ADS ($\sum Q_{ADS}^{AMG}$), reactive power loss ($\sum Q_{ADS}^{Loss}$), and the DRPs reactive power withdrawal/injection from/to the ADS ($\pm \sum Q_{ADS}^{DRP}$) for each interval of simulation.

A. CHP, Boiler, TES and ESS constraints:

The TES constraints are maximum capacity, charge and discharge constraints, and mass balance constraints and boiler constraints are available in [33].

B. SWT and PVA constraints:

The SWT equation is [30]:

$$P^{SWT} = \begin{cases} 0 & if\ v^{Wind} \le v_c^{Wind}\ or\ v^{Wind} \ge v_f^{Wind} \\ P_r^{Wind} \cdot \dfrac{(v^{Wind} - v_c^{Wind})}{(v_r^{Wind} - v_c^{Wind})} & if\ v_c^{wind} \le v^{Wind} \le v_r^{wind} \\ P_r^{Wind} & otherwise \end{cases} \quad (10)$$

The maximum electricity output of PVA is [33]:

$$P^{PVA} = A^{PVA}.\xi.I.(1 - 0.005.(t_0 - 25)) \quad (11)$$

Eq. (11) terms are the PVA area (A^{PVA}), energy conversion efficiency (ξ), the solar irradiation (I), and the outside air temperature (t_0), respectively.

C. DRP constraints:

The ADS can contract with the ADS to perform DLC procedure by paying a predefined fee. Thus, the ADS controllable loads can be dispatched by the ADS in the DLC program. Hence, the DRP constraints are [33]:

$$P^{Load} = P_{Critical}^{Load} + P_{Controllable}^{Load} \quad (12)$$

$$\Delta P_{Min}^{DLC} \le \Delta P^{DLC} \le \Delta P_{Max}^{DLC},\ \Delta P_{Max}^{DLC} = P_{Controllable}^{Load} \quad (13)$$

$$P^{DRP} = \Delta P^{DLC} \quad (14)$$

Eq. (12) terms the ADS critical electrical load ($P_{Critical}^{Load}$) and controllable electrical load ($P_{Controllable}^{Load}$), respectively. Eq. (13) presents the maximum and minimum limits of DLC control variables. Further, Eq. (13) considers that the maximum value of DLC control variable (ΔP_{Max}^{DLC}) is equal to the controllable electrical load. Eq. (14) denotes that the value of DRP power is equal to the DLC variable.

D. Electric network constraints:

A. Steady-state security constraints:

$$\sqrt{P_{nm}{}^2(V,\delta)+Q_{nm}{}^2(V,\delta)} \le F_{nm}^{\max} \tag{15}$$

$$V_n^{\min} \le |V_n| \le V_n^{\max} \tag{16}$$

Eq. (15) terms are the active ($P_{nm}{}^2(V,\delta)$) and reactive power ($Q_{nm}{}^2(V,\delta)$) of distribution feeders. $F_{nm}^{\max}$ is the maximum permissible flow limit of distribution feeder. Eq. (16) is the minimum and maximum value limits of the ADS bus voltage.

2) Maximum apparent power for exchanging with the upstream network:

$$\sqrt{P_{jt}^2+Q_{jt}^2} \le F_j^{\max-upstream} \ \forall j, \ \forall t \tag{17}$$

Eq. (17) terms are the active (P_{jt}^2) and reactive power (Q_{jt}^2) of Point of Common Coupling (PCC). The $F_j^{\max-upstream}$ parameter is the maximum volt-ampere capacity of the PCC.

The integrated constraints of the first level optimization problem can be represented as:

$$Z_1(x,u,z)=0 \tag{18}$$

$$\Upsilon_1(x,u,z)\le 0 \tag{19}$$

2.3. AMGs DA Optimization Problem Formulation

The AMG proposes the bid/offer of energy and reactive power to the ADSO:

$$Max\ \mathsf{M}_2 = \sum_{NAMGS} prob.\begin{pmatrix} -C_{AMG}^{CHP}-C_{AMG}^{DG}-C_{AMG}^{Boiler}-C_{AMG}^{ESS}-C_{AMG}^{PHEV} \\ -C_{AMG}^{TES}-C_{AMG}^{Purchase}+B_{AMG}^{Sell}+B_{AMG}^{DRP} \end{pmatrix} \tag{20}$$

The Eq. (20) components are AMG's DERs costs and DRP and the energy and ancillary services sold revenues. The objective function is divided into nine terms: 1) the cost of CHP (C_{AMG}^{CHP}); 2) the cost of DG (C_{AMG}^{DG}); 3) the cost of boiler (C_{AMG}^{Boiler}); 4) the cost of ESS (C_{AMG}^{ESS}); 5) the cost of PHEV (C_{AMG}^{PHEV}); 6) the cost of TES (C_{AMG}^{TES}); 7) the energy purchasing cost ($C_{AMG}^{Purchase}$); 8) the benefit of energy and ancillary services sold to the ADS (B_{AMG}^{Sell}); and 9) the benefit of DRP implemented by the ADS (B_{AMG}^{DRP}).

The revenue of AMG can be written as (21):

$$B_{AMG}^{Sell}=\left(\sum\lambda^{active}.P_{DA\_ADS}^{active}+\sum\lambda^{SR}.SR_{DA\_ADS}+\sum\lambda^{reactive}.Q_{DA\_ADS}^{reactive}\right) \tag{21}$$

Eq. (21) terms are the AMGs active power sold to the ADS in the DA market ($\sum\lambda^{active}.P_{DA\_ADS}^{active}$), the AMGs spinning reserve sold to the ADS in the DA market ($\sum\lambda^{SR}.SR_{DA\_ADS}$), and the AMGs reactive power sold to the ADS in the DA market ($\sum\lambda^{reactive}.Q_{DA\_ADS}^{reactive}$) for each interval of simulation.

Electric power balance constraint of AMG is given by:

$$P_{AMG}^{Total}=(-\sum P_{AMG}^{Load}+\sum P_{AMG}^{PVA}+\sum P_{AMG}^{ESS}+\sum P_{AMG}^{SWT}+\sum P_{AMG}^{CHP}+\sum P_{AMG}^{DG} + \sum P_{AMG}^{DRP}+\sum P_{AMG}^{PHEV}-P_{AMG}^{Loss}) \tag{22}$$

$$Q_{AMG}^{Total}=(-\sum Q_{AMG}^{Load}+\sum Q_{AMG}^{DRP}-Q_{AMG}^{Loss}+\sum Q_{AMG}^{DG}) \quad (23)$$

Eq. (22) terms are the active power withdrawal of load ($-\sum P_{AMG}^{Load}$), the DERs active power injection to the AMG ($\sum P_{AMG}^{PVA}+\sum P_{AMG}^{ESS}+\sum P_{AMG}^{SWT}+\sum P_{AMG}^{CHP}+\sum P_{AMG}^{DG}+\sum P_{AMG}^{DRP}+\sum P_{AMG}^{PHEV}$), and active power loss ($\sum P_{AMG}^{Loss}$) for each interval of simulation. Further, Eq. (23) terms are the reactive power withdrawal of load ($\sum Q_{AMG}^{Load}$), the DRP reactive power injection to the AMG ($\sum Q_{AMG}^{DRP}$), reactive power loss (Q_{AMG}^{Loss}), and reactive power injection to the AMG ($\sum Q_{AMG}^{DG}$) for each interval of simulation.

The heating power balance constraint is (24):

$$-\sum Q'^{Load}_{AMG}+\sum Q'^{B}_{AMG}+\sum Q'^{CHP}_{AMG}-Q'^{Loss}_{AMG}=0 \quad (24)$$

Eq. (24) terms are the heating loads ($\sum Q'^{Load}_{AMG}$), the boilers and CHP heating power injection to the AMG ($\sum Q'^{B}_{AMG}+\sum Q'^{CHP}_{AMG}$), and heating power loss (Q'^{Loss}_{AMG}) for each interval of simulation.

A. DRP constraints:

The AMG loads consist of critical, deferrable and controllable loads.

$$P_{AMG}^{Load}=P_{\text{AMG }Critical}^{Load}+P_{\text{AMG }Deferrable}^{Load}+P_{\text{AMG }Controllable}^{Load} \quad (25)$$

$$\Delta P_{AMG}^{TOU}=P_{\text{AMG }Deferrable}^{Load} \quad (26)$$

$$\sum_{t=1}^{Period}\Delta P_{AMG}^{TOU}=0 \quad (27)$$

$$\Delta P_{\text{AMG }Min}^{TOU}\le\Delta P_{AMG}^{TOU}\le\Delta P_{\text{AMG }Max}^{TOU} \quad (28)$$

$$\Delta P_{\text{AMG }Min}^{DLC}\le\Delta P_{AMG}^{DLC}\le\Delta P_{\text{AMG }Max}^{DLC},\ \Delta P_{\text{AMG }Max}^{DLC}=P_{\text{AMG }Controllable}^{Load} \quad (29)$$

$$P_{AMG}^{DRP}=\Delta P_{AMG}^{DLC}+\Delta P_{AMG}^{TOU} \quad (30)$$

Eq. (25) terms the AMG critical electrical load ($P_{\text{AMG }Critical}^{Load}$), deferrable load ($P_{\text{AMG }Deferrable}^{Load}$), and controllable electrical load ($P_{\text{AMG }Controllable}^{Load}$), respectively. Eq. (26) denotes that the change of TOU power is equal to the deferrable load. Further, Eq. (27) considers that the sum of the TOU power changes is equal to zero. Thus, all of the deferrable load should be supplied in the operational horizon.

Eq. (28) and Eq. (29) present the maximum and minimum limits of TOU and DLC electrical power variables, respectively. Further, Eq. (29) considers that the maximum value of DLC control variable ($\Delta P_{AMG\ Max}^{DLC}$) is equal to the AMG controllable electrical load. Finally, Eq. (30) denotes that the sum of the AMG demand response program active power equals to the sum of the changes of the active power of DLC and active power of TOU.

The energy purchased costs and energy sold benefits are given by (31) and (32):

$$If\ P^{AMG}>0\ Then\ B_{Sell}^{AMG}=P^{AMG}.\kappa_{Sell}^{Elect}\ else\ C_{Purchase}^{AMG}=P^{AMG}.\kappa_{Purchased}^{Elect} \quad (31)$$

$$B_{DRP}^{AMG}=\Delta P_{AMG}^{TOU}.\kappa_{TOU}^{Elect}+\Delta P_{AMG}^{DLC}.\kappa_{DLC}^{Elect} \quad (32)$$

Eq. (31) denotes that if the AMG sells the electricity to the ADS, then the benefit of the AMG equals to $B_{Sell}^{AMG}=P^{AMG}.\kappa_{Sell}^{Elect}$. The P^{AMG} variable is the active power sold to the ADS and the κ_{Sell}^{Elect} parameter is the electricity

selling price. If the AMG purchases the electricity from the ADS, then the purchasing cost of the AMG equals to $C^{AMG}_{Purchase} = P^{AMG}.\ \kappa^{Elect}_{Purchased}$ and the $\kappa^{Elect}_{Purchased}$ parameter is the electricity purchasing price. Further, Eq. (32) denotes that the benefit of the DRP implementation for the AMG equals to the sum of the benefits of the TOU and DLC programs. The κ^{Elect}_{TOU}, κ^{Elect}_{DLC} parameters are the price of TOU and DLC implementation, respectively.

B. PHEV model and constraints:

The energy balance is given as (33) and (34), respectively [34]:

$$ENPHEV(t) = ENPHEV(t-1) + \varpi^{Charge}_{PHEV}.PCH^{PHEV}(t).\Delta t - \frac{1}{\varpi^{Discharge}_{PHEV}}.PDCH^{PHEV}.\Delta t \quad (33)$$

$$ENPHEV^{min} \le ENPHEV \le ENPHEV^{max} \quad (34)$$

$$0 \le PCH^{PHEV} \le PCH^{PHEV,Max} \quad (35)$$
$$0 \le PDCH^{PHEV} \le PDCH^{PHEV,Max}$$

$$ENPHEV(t) = \sigma.ENPHEV^{max} \quad \forall\ t = t_{Departure} \quad (36)$$

Eq. (31) denotes that the energy balance of PHEV battery for each interval of simulation that the ϖ^{Charge}_{PHEV} and $\varpi^{Discharge}_{PHEV}$ parameters are the charge and discharge limitation ratio, respectively. The PCH^{PHEV} and $PDCH^{PHEV}$ variables are the PHEV's power of charge and discharge, respectively.
The limits of charge and discharge rates of PHEV battery are presented in Eq. (35). Eq. (36) denotes that the desired PHEV state of charge at the leaving time and the σ parameter is the expected coefficient.

2.4. ADS DA Contingency Constrained Topology Optimization Problem Formulation

At the third level of the optimization problem, the ADS day-ahead contingency constrained topology optimization problem is considered. At this level, the third level of uncertainty modelling is used, the contingency scenarios are considered, and the corrective DRPs and involuntary load interruptions are determined. The objective function of the problem can be written as:

$$Min\ \mathsf{M}_3 = -\mathsf{M}_1 + \sum_{NCSS} \gamma.P_{shed}.\ CDF \quad (37)$$

The constraints of this problem are presented as:

$$P_{shed} \le P^{Max}_{shed} \quad (38)$$

Eq. (31) considers the maximum limit of shed load.

2.5. ADS RT Optimization Problem Formulation

The fourth level problem minimizes the operation costs of ADS resources in the RT market. At the real-time optimization problem, the look-ahead approach or predictive control model is used as described in [7]. The optimization algorithm is performed for every 15 minutes with updated forecasted data for active and reactive power markets as shown in Fig. 4.

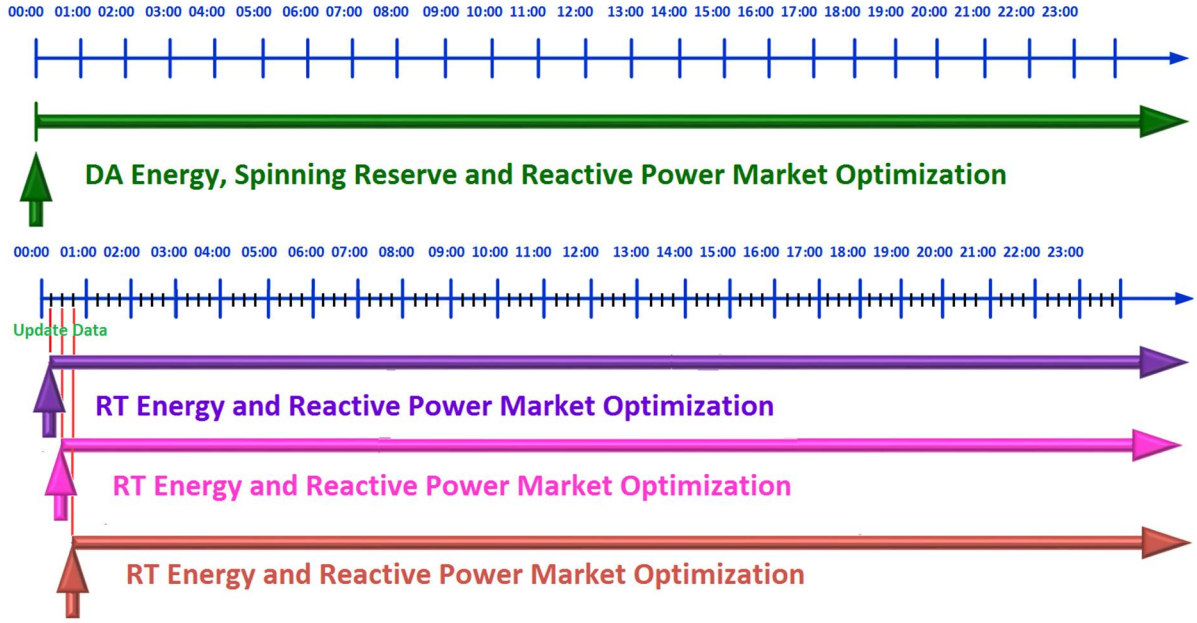

Fig. 4. The ADSO day-ahead and real-time OBSADS horizon.

As described in the modeling section, the accepted spinning reserve bids in DA market must be controlled as fixed parameters in the RT markets and any deviation of spinning reserve parameters are penalized by the upward market operator. The objective of each real-time optimization is and can be represented as [7]:

$$Min\ \mathsf{M}_4 = \sum_{NOSS} prob. \sum_{NCSS} prob. \sum_{T+1} \left(\begin{array}{l} W_3[(\Delta C_{ADS}^{CHP} + \Delta C_{ADS}^{DG} + \Delta C_{ADS}^{ESS} + \Delta C_{ADS}^{TES} + \Delta C_{ADS}^{Boiler}) \\ + \Delta C_{ADS}^{Purchase} + \Delta C_{DRP}^{AMG} + (\sum Penalty^{active} + \\ \sum Penalty^{reactive}) - \Delta revenue] + W_4.(\sum_{NL} \Delta LMP.\Delta P_L - \sum_{NG} \Delta LMP.\Delta P_G) \end{array} \right) \quad (39)$$

$$s.t.: \quad Z'^{\alpha}_{RT\_ADS}(x,u,z,t) = 0 \qquad \forall \alpha \in \{0,1,....,NCSS\}$$
$$\Upsilon'^{\alpha}_{RT\_ADS}(x,u,z,t) \le 0$$

$$\Delta revenue = \left(\begin{array}{l} \sum \lambda_{RT}^{active}.(P_{RT\_upward}^{active} - P_{DA\_upward}^{active}) + \sum \lambda_{RT}^{SR}.(SR_{RT\_upward} - SR_{DA\_upward}) \\ + \sum \lambda_{RT}^{reactive}.(Q_{RT\_upward}^{reactive} - Q_{DA\_upward}^{reactive}) + \sum \eta_{RT\_downward}^{active}.(P_{RT\_downward}^{active} - P_{DA\_downward}^{active}) \\ + \sum \eta_{RT\_downward}^{reactive}.(Q_{RT\_downward}^{reactive} - Q_{DA\_downward}^{reactive}) \end{array} \right) \quad (40)$$

Eq. (39) is divided into five groups: 1) the mismatch of commitment costs of ADS' DERs consist of CHP, DG, ESS, TES, and boiler $(\Delta C_{ADS}^{CHP} + \Delta C_{ADS}^{DG} + \Delta C_{ADS}^{ESS} + \Delta C_{ADS}^{TES} + \Delta C_{ADS}^{Boiler})$; 2) the mismatch cost of energy purchased from wholesale market $(\Delta C_{ADS}^{Purchase})$; 3) the mismatch costs of AMGs' DRPs (ΔC_{DRP}^{AMG}); 4) the mismatch of penalty of deviation in active and reactive markets $(\sum Penalty^{active} + \sum Penalty^{reactive})$; 4) the mismatch of revenues $(\Delta revenue)$; and 5) the mismatch of weighted difference of the LMP of load and generation buses $(\sum_{NL} \Delta LMP.\Delta P_L - \sum_{NG} \Delta LMP.\Delta P_G)$.

Further, Eq. (40) is divided into five groups: 1) the revenue of active power mismatch sold to the RT upward market $(\sum \lambda_{RT}^{active}.(P_{RT\_upward}^{active} - P_{DA\_upward}^{active}))$; 2) the revenue of spinning reserve mismatch sold to the RT upward market $(\sum \lambda_{RT}^{SR}.(SR_{RT\_upward} - SR_{DA\_upward}))$; 3) the revenue of reactive power mismatch sold to the RT upward market

$(\sum \lambda_{RT}^{reactive}.(Q_{RT\_upward}^{reactive} - Q_{DA\_upward}^{reactive}))$; 4) the revenue of active power mismatch sold to the downward customers in RT market horizon $(\sum \eta_{RT\_downward}^{active}.(P_{RT\_downward}^{active} - P_{DA\_downward}^{active}))$; and 5) the revenue of reactive power mismatch sold to the downward customers in RT market horizon $\sum \eta_{RT\_downward}^{reactive}.(Q_{RT\_downward}^{reactive} - Q_{DA\_downward}^{reactive})$.

2.6. AMG RT Market Optimization Problem Formulation

The fifth level problem minimizes the mismatch of operation costs of AMG resources in the RT market. Same as the fourth level, the look-ahead approach is used as described in [7] and the objective function of the fifth-level problem can be represented as:

$$Min\ \mathsf{M}_5 = \sum_{NOSS} prob. \sum_{NCCS} prob. \sum_{T+1} \begin{pmatrix} \Delta C_{AMG}^{CHP} + \Delta C_{AMG}^{DG} + \Delta C_{AMG}^{ESS} + \Delta C_{AMG}^{TES} + \Delta C_{AMG}^{PHEV} \\ + \Delta C_{AMG}^{Boiler} + \Delta C_{AMG}^{Purchase} - \Delta B_{AMG}^{Sell} - \Delta B_{AMG}^{DRP} \\ \sum Penalty^{active} + \sum Penalty^{reactive} \end{pmatrix} \tag{41}$$

$$s.t.: \quad Z_{RT\_AMG}^{'\alpha}(x,u,z,t) = 0 \qquad \forall \alpha \in \{0,1,....,NCSS\}$$
$$\Upsilon_{RT\_AMG}^{'\alpha}(x,u,z,t) \le 0$$

The Eq. (41) components are the AMG's DERs mismatch of costs, DRP and energy sold to ADS mismatch of benefits, and the active and reactive power mismatch penalties.

Where $Z_{RT\_AMG}(x,u,z)=0$ and $\Upsilon_{RT\_AMG}(x,u,z)\le 0$ are fourth level problem constraints.

2.7. ADS RT Contingency Constrained Topology Optimization Problem Formulation

At the sixth level problem, the ADS RT contingency constrained topology optimization problem is considered. At this level, the data is updated and corrective DRPs and involuntary load interruptions are determined. The objective function of the sixth level problem can be written as:

$$Min\ \mathsf{M}_6 = -\mathsf{M}_5 + \sum_{NOCS} \gamma.P_{shed}.CDF \tag{42}$$

The sixth level objective function minimizes the fifth-level problem objective function and the involuntary load shedding. The constraints of this problem are presented as:

$$P_{shed} \le P_{shed}^{Max} \tag{43}$$

The proposed MINLP model of OBSADS is a non-convex, non-linear optimization problem. The optimization algorithm is given in Fig. 5.

3. Optimization algorithm

The optimization problem assumes:

- The upward day-ahead market energy, spinning reserve and reactive power services prices are forecasted by Ref. [35] model for each scenario of the first stage of uncertainty modeling.
- The hourly heating and electrical loads are forecasted by the ARIMA model for each scenario of the second stage of uncertainty modeling [33].
- Numerous scenarios for day-ahead market energy, spinning reserve, reactive power services prices, hourly heating and electrical loads are generated [36].
- A Monte Carlo simulation method is utilized for the third stage of uncertainty modeling. The domain of contingency scenarios is defined and then, it generates contingency scenarios randomly from the domain using a certain specified probability distribution [33].
- All of the weighting factors are equal to 1.
- The confidence level used to calculate $CVaR_\alpha$ is $\alpha = 0.95$.

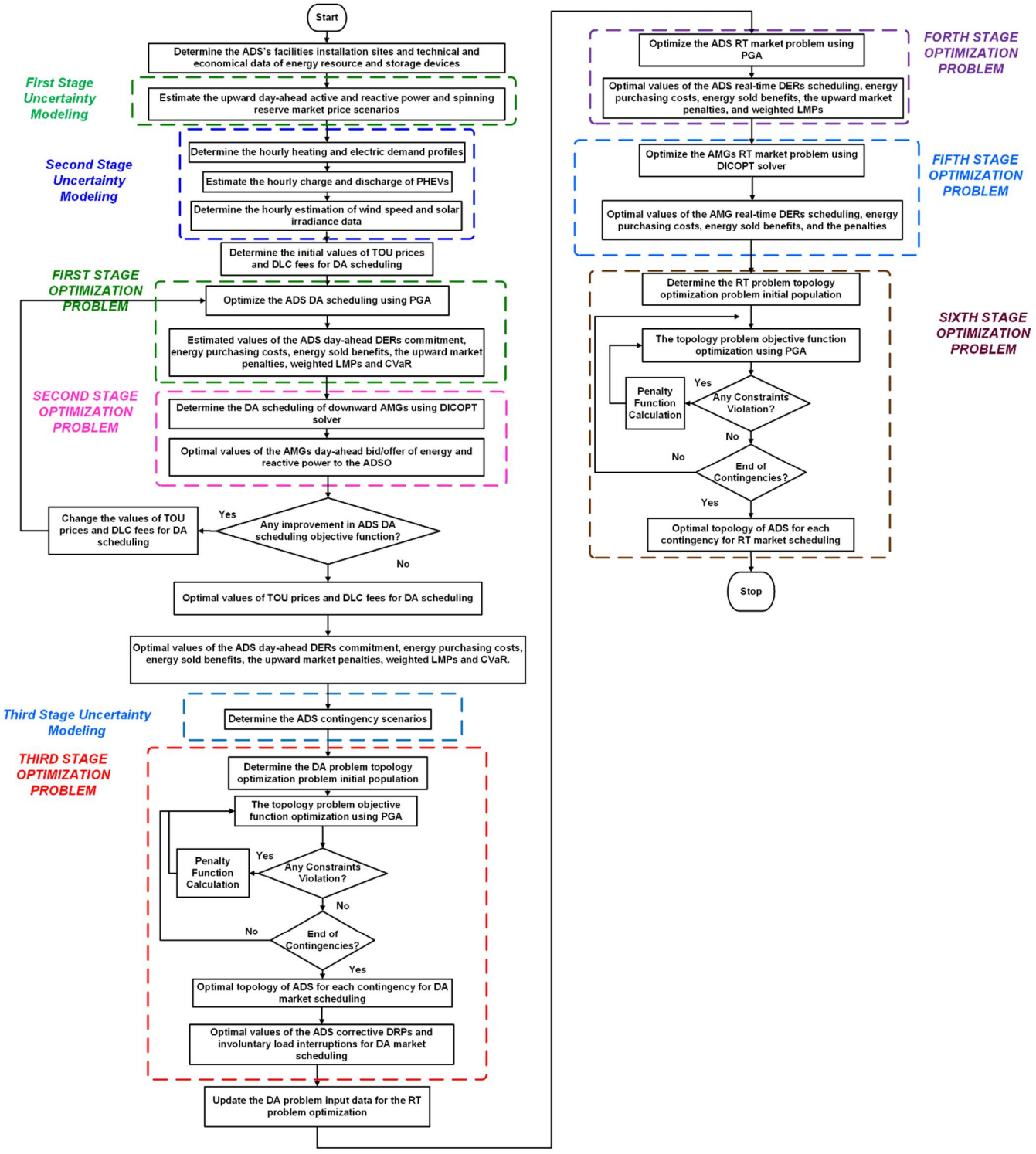

Fig. 5. Flowchart of the OBSADS algorithm.

- The 1st, 3rd, 4th, and 6th level optimization problems are MINLP and are solved by the Parallel Genetic Algorithm (PGA) that all of the details of the algorithm is presented in [37].
- The DICOPT solver of GAMS is used for the 2nd and 5th level problems.
- The Capacitor Bank (CB) steps and tie-switches control variables are assumed as discrete control variables.
- The 1st – 3rd level problems use the hourly load curves. The 4th – 6th level problems use the ARIMA forecasting model with the 1-minute resolution.
- An index is proposed as the Average Zonal LMP Deviation (AZLMPD) with the following formulation for the normal and the worst-case contingent condition of the ADS:

$$AZLMPD = \sum_{t=1}^{24} \frac{ZLMP^{Max} - ZLMP^{Min}}{AZLMP} \quad (44)$$

Where, $ZLMP^{Max}$ and $ZLMP^{Min}$ are maximum and minimum zonal LMP, respectively. $AZLMP$ is the hourly average of zonal LMP for the specified time horizon.

- The corrective load shedding (CLS) uses the following algorithm:
  - At first, the AMG's controllable loads ($P_{Controllable}^{Load}$) are turned off,
  - If the electric power balance constraint is not satisfied, then turn off the whole zonal load block and P_{shed} is the total shed load.

The parallel genetic algorithm codes were developed in MATLAB and the simulation was carried out on a PC (Intel Core i7-870 processor, 4*2.93 GHz, 8 GB RAM). The parallel processing functions of MATLAB was utilized to speed up the computation time. The maximum CPU time required solving the entire problem was less than 372 seconds. The computation times of the 2nd and 5th level problems were less than 53 seconds.

The DICOPT solver of GAMS is used for the 2nd and 5th level problems. The DICOPT (DIscrete and Continuous OPTimizer) solver iteratively utilizes the CPLEX and CONOPT3 solvers for Non-Linear Programming (NLP) and Mixed Integer Programming (MIP) solutions, respectively.

4. Simulation Results

The 123-bus test system data is presented in [38] and its topology is shown in Fig. 6. The AMG was the 33-bus test system [39]. Fig. 7 depicts the estimated hourly electrical and heating loads of 123-bus system.
Fig. 8 depicts the estimated value of energy and ancillary services prices for the day-ahead and real-time markets for one of the reduced scenarios. The simulation results of two cases are considered: without OBSADS procedure and with OBSADS procedure.

4.1. Case 1: Without OBSADS procedure

In this case, the 123-bus ADS only transacts energy and reactive power with the upward market. Further, the ADSO does not utilize DRP alternatives. The AMGs submits their active and reactive bids without consideration of the second level of OBSADS procedure and there is not any reconfiguration optimization after the ADS contingencies. Thus, any critical contingency imposes load-shedding procedure and customer interruption costs to the ADSO. The W and β parameters are equal to zero.
Fig. 9 depicts the aggregated AMGs bid/offer values of active power, the 123- bus active load, the 123-bus system DERs active power generation and the bid/offer values of the active power of 123- bus system ADS, respectively. The AMGs propose electricity injection for 08:00 PM to 06:00 AM and electricity withdrawal for 07:00 AM to 07:00 PM, respectively. The maximum and minimum value of the ADS active power take on a value 6398.85 (kW) and -4873.31 (kW), respectively.
Fig. 10 depicts the aggregated AMGs bid/offer values of reactive power, the 123- bus reactive load, the 123-bus system DERs reactive power generation and the bid/offer values of reactive power of 123- bus system ADS, respectively. The AMGs propose reactive power injection for 08:00 PM to 05:00 AM and electricity withdrawal for 06:00 AM to 07:00 PM, respectively. The maximum and minimum value of the ADS reactive power take on a value 5967.29 (kW) and -1021.45 (kW), respectively.
Fig.11 shows the worst-case of the ADS PVAs and SWTs electricity generation. Fig. 12. (a) and (b) show the electricity and heating dispatch of the 123-bus system CHPs, respectively. The CHPs were at full load when they committed.
Fig. 13. shows the boilers heating dispatch of the 123-bus system. The boilers track the heating load and compensate the mismatch of heating load and heating generation of CHPs.

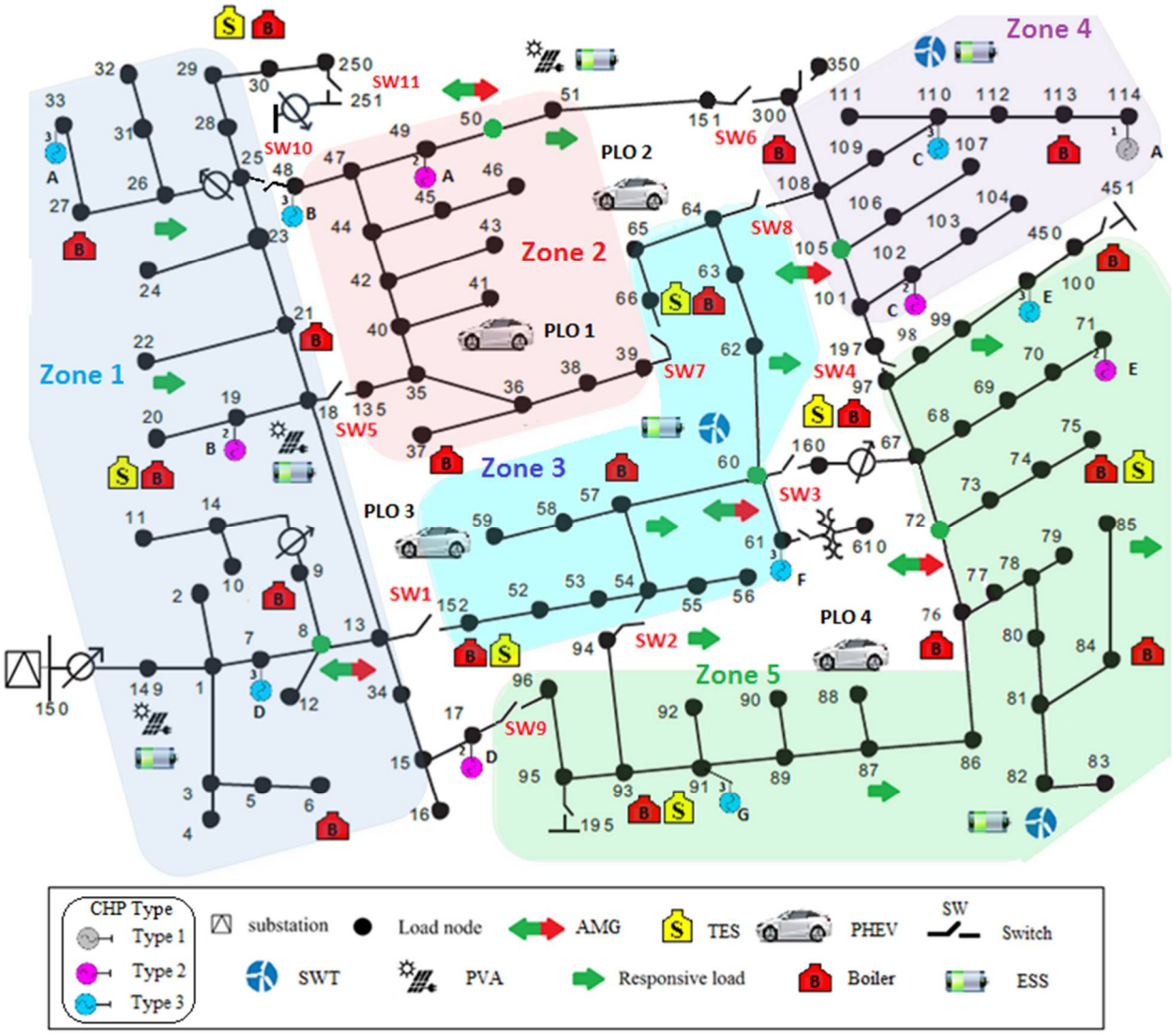

Fig.6. The modified 123-bus ADS test system.

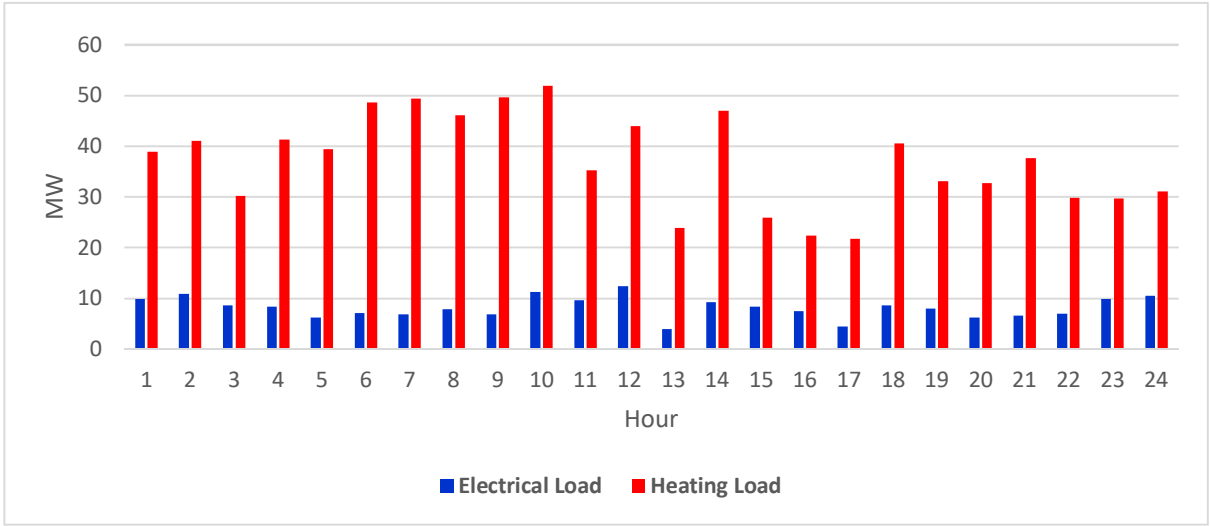

Fig.7. The hourly heating and electrical loads of the 123-bus test system.

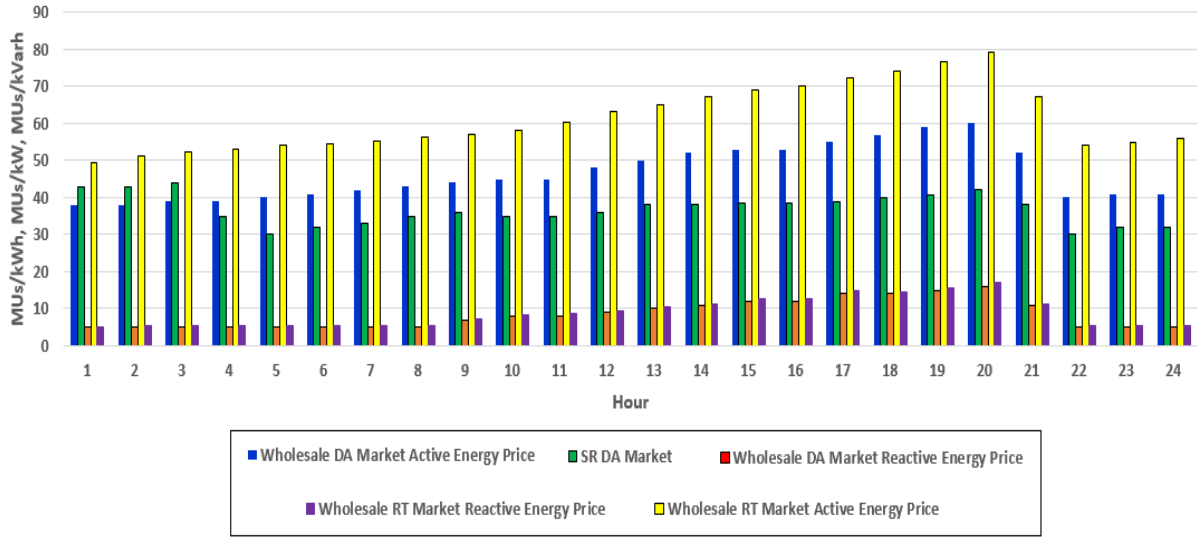

Fig. 8. The estimated value of energy and ancillary services prices for the day-ahead and real-time markets for one of the reduced scenarios.

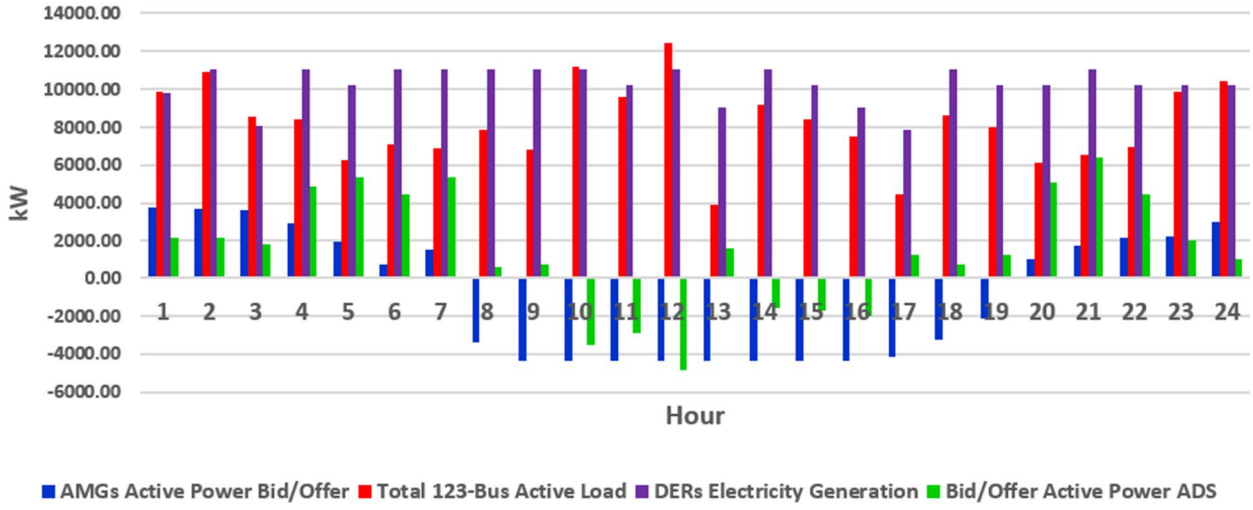

Fig. 9. The aggregated AMGs bid/offer values of active power, the 123- bus active load, the 123-bus system DERs electricity generation and the bid/offer values of active power of 123- bus system ADS.

Fig. 10. The aggregated AMGs bid/offer values of reactive power, the 123- bus reactive load, the 123-bus system DERs reactive power generation and the bid/offer values of reactive power of 123- bus system ADS.

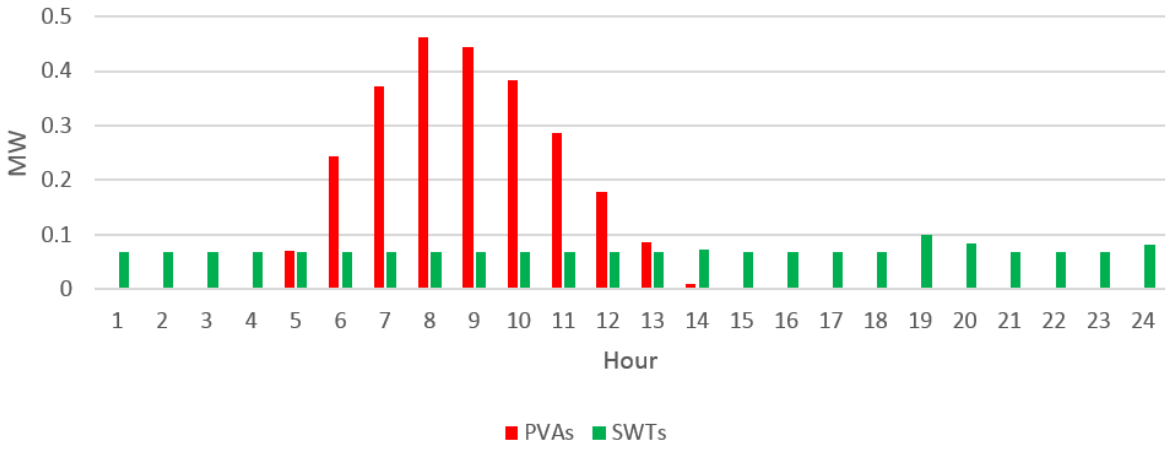

Fig.11. The worst case of the ADS's PVAs and SWTs electricity generation.

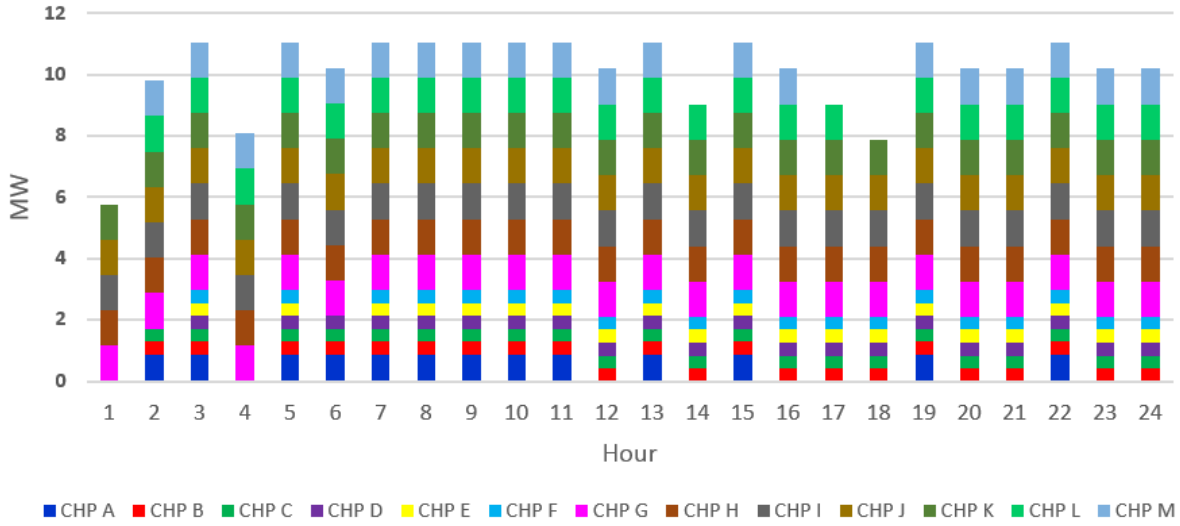

(a)

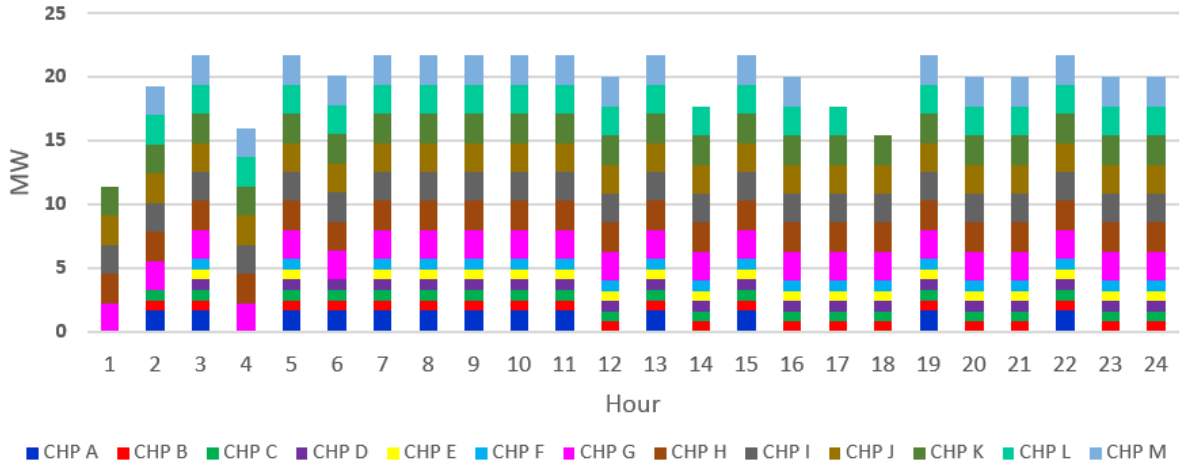

(b)

Fig. 12. (a) The CHPs electricity dispatch of the 123-bus system. (b) The CHPs heating dispatch of the 123-bus system.

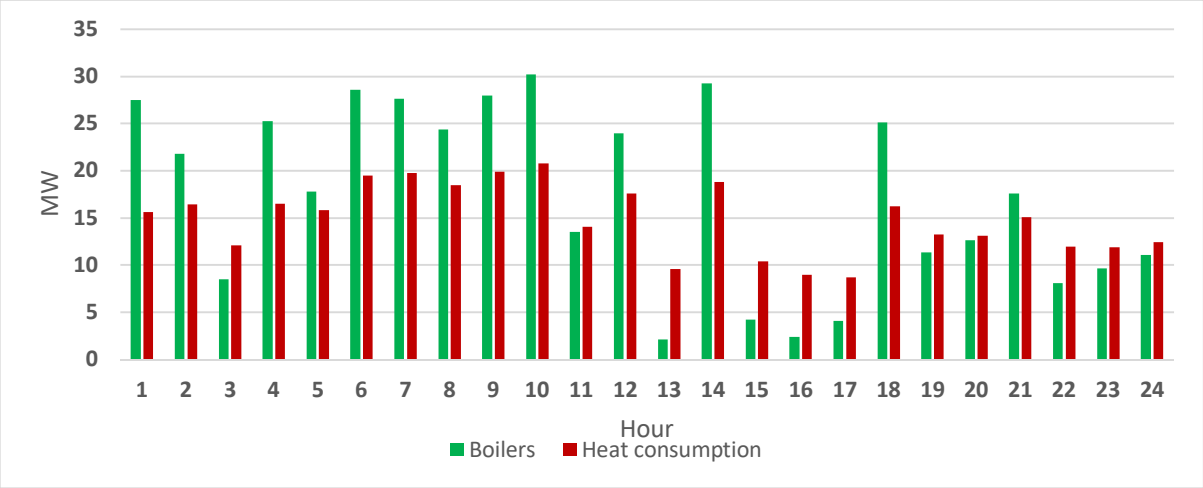

Fig. 13. The boilers heating dispatch of the 123-bus system.

Fig. 14. depicts the values of AMGs bids/offers and AMGs accepted bids/offers. The maximum and minimum value of the AMGs bid/offer are 4331.95 (kW) and -4909.35 (kW) that belong to the AMG5 for 01:00 AM and 09:00 AM – 06:00 PM, respectively. The maximum and minimum value of the accepted AMGs bid/offer are 1025.68 (kW) and -1178.35 (kW) that belong to the AMG2 (for 03:00 AM) and the AMG1 (for 08:00 AM – 06:00 PM), respectively. Fig. 15 depicts the expected benefit/cost of 123- bus system ADS for bid/offer values of DA energy and reactive markets. The total benefit of ADS takes on the value 70918.16 (MU/Day) for the first case study.

4.2. Case 2: Considering OBSADS procedure

In this case, the ADS utilizes the OBSADS procedure and it participates in the upward wholesale energy, spinning reserve and reactive power markets.

Fig.16 shows two scenarios of time of use and DLC that are considered in the OBSADS procedure and the best scenario of DRP is selected in the following case study.

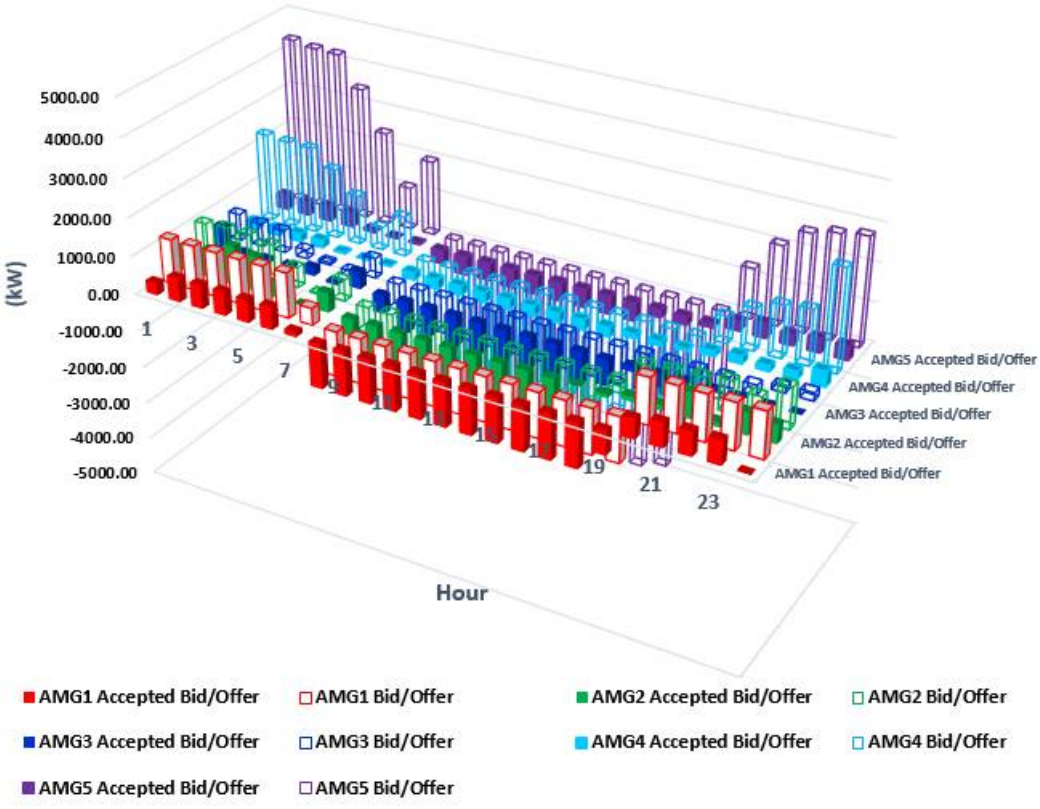

Fig. 14. The values of AMGs bids/offers and AMGs accepted bids/offers.

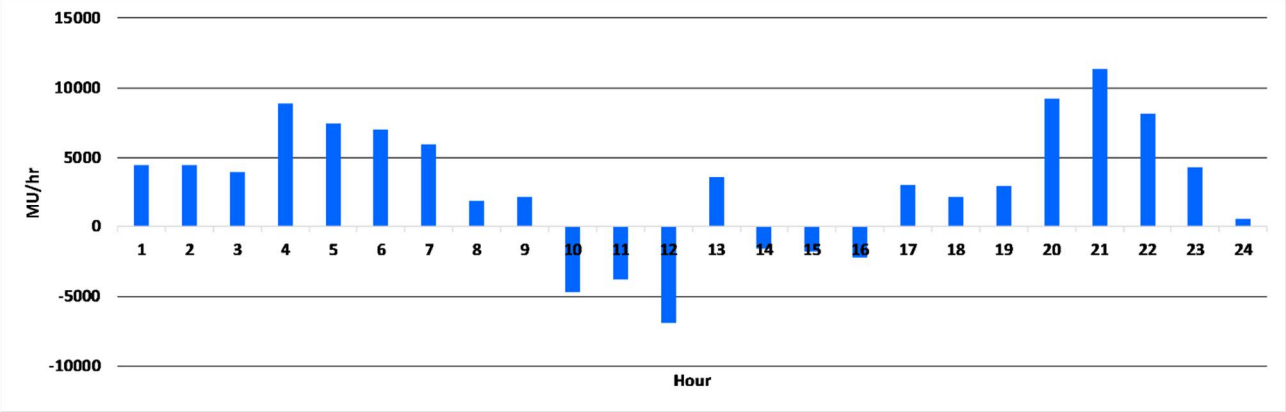

Fig. 15. The expected benefit/cost of 123- bus system ADS for DA markets of energy and reactive power.

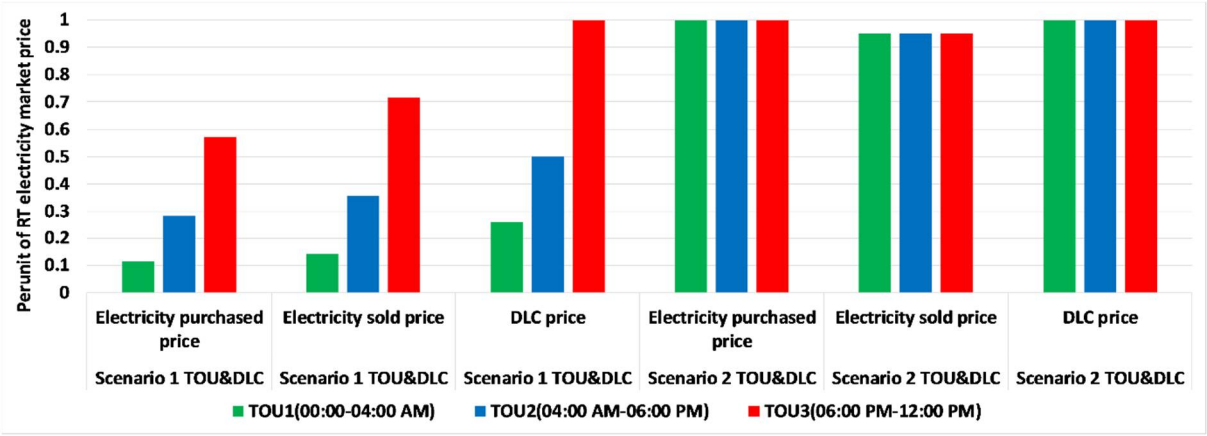

Fig. 16. Two scenarios of TOU and DLC

As shown in Fig. 16, the electricity sold price and DLC prices are equal for the second scenario of time of use and DLC; meanwhile, the electricity purchased price of this scenarios is about 95 percent of its electricity sold price.

Fig. 17 depicts the aggregated AMGs bid/offer values of active power, the 123- bus active load, the 123-bus system DERs active power generation and the bid/offer values of the active power of 123- bus system ADS for β=1, respectively. The AMGs proposes electricity injection for 03:00 PM to 08:00 AM and electricity withdrawal for 09:00 AM to 02:00 PM, respectively. The maximum and minimum value of the ADS active power take on a value 6961.56 (kW) and -2664.63 (kW), respectively. In this case, the ADS submitted value of active power is about 8.06% more than the first case. The second scenario of time of use and DLC is selected as the best of DRP alternatives by the OBSADS. Fig. 18 depicts the aggregated AMGs bid/offer values of reactive power, the 123- bus reactive load, the 123-bus system DERs reactive power generation and the bid/offer values of reactive power of 123- bus system ADS for β=1, respectively. The maximum and minimum value of the ADS reactive power take on a value 4967.29 (kVAr) and -2021.45 (kW), respectively. Fig. 19. (a) and (b) show the electricity and heating dispatch of the 123-bus system CHPs for β=1, respectively. The CHPs were at full load when they committed.

Fig. 20 shows the boilers heating dispatch of the 123-bus system for β=1. The boilers track the heating load and compensate the mismatch of heating load and heating generation of CHPs. Fig. 21 depicts the values of AMGs bids/offers and AMGs accepted bids/offers. The maximum and minimum value of the AMGs bid/offer are 4743.31 (kW) and -1378.43 (kW) that are belong to the AMG5 for 01:00 AM and 11:00 AM, respectively. The maximum and minimum value of the accepted AMGs bid/offer are 1723.97 (kW) and -621.65 (kW) that belong to the AMG5 (for 08:00 AM) and the AMG1 (for 09:00 AM – 06:00 PM), respectively.

Fig. 22 depicts the charge and discharge of PHEVs for OBSADS and without OBSADS cases. When the ADS participates in spinning reserve market and it considers the OBSADS, the PHEVs' batteries are more discharged. Fig. 23 depicts the bid/offer values of (a) active power, (b) spinning reserve and, (c) reactive power of 123- bus

system ADS for different values of β, respectively. As shown in Fig. 23, as the value of β is increased, the absolute values of ADS bids/offers are decreased based on the fact that the ADSO chooses a risk-averse bidding strategy.
Table 2 shows the optimal switching device status for the normal and some of the zonal worst-case contingent conditions of the 123-bus test system that are consist of the first five ranks of the worst-case zonal contingent conditions. The optimization procedure searches the state space of the problem and switches the switching devices; meanwhile, it optimizes the dispatchable DERs of the system.
Fig. 24 shows the estimated hourly average zonal LMP values for (a) normal condition, (b) Fault: L60-62 (Zone 3), and (c) Fault: L13-18 (Zone 1) contingent conditions of the 123-bus test system for β=1.
As shown in Fig. 23. (a), the range of zonal LMP values is between 40.1 (MU/hr) – 58.2 (MU/hr). However, for the Fault: L60-62, the range of zonal LMP values are changed to 46.1 (MU/hr) – 78.2 (MU/hr). Finally, for the Fault: L13-18 as one of the worst contingencies, the range of zonal LMP values are 47.2 (MU/hr) – 81.2 (MU/hr).
At the real-time optimization problem, the predictive control model is used and the 15 minutes updated data are used for the optimization algorithm [7].

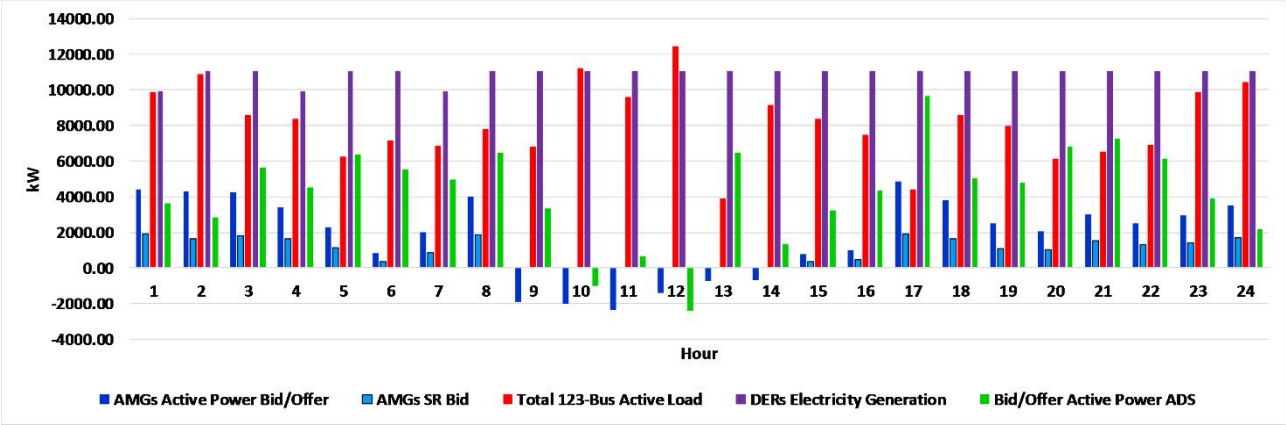

Fig. 17. The aggregated AMGs bid/offer values of active power, the 123-bus active load, the 123-bus system DERs electricity generation and the bid/offer values of the active power of 123-bus system ADS for β=1.

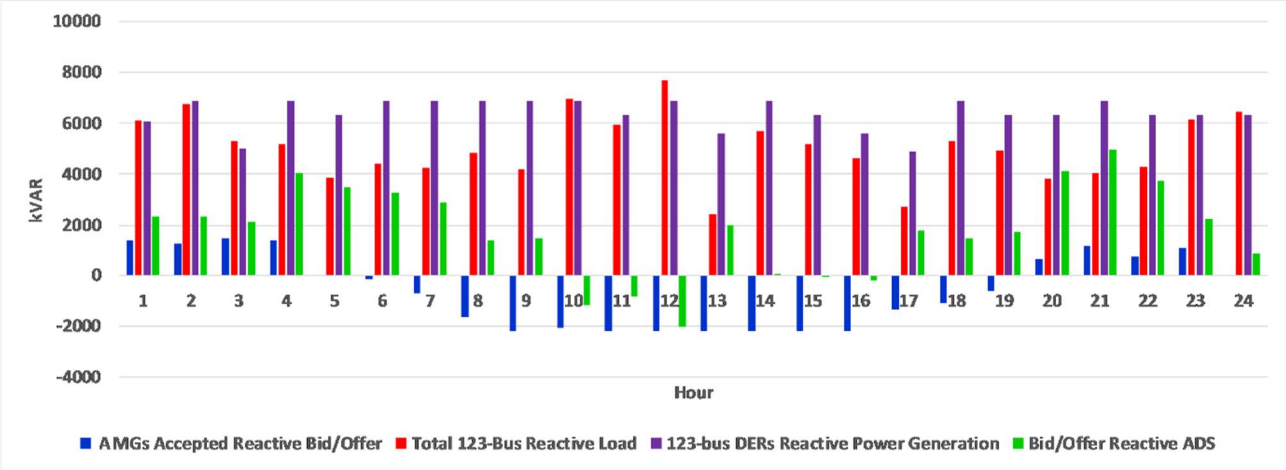

Fig. 18. The aggregated AMGs bid/offer values of reactive power, the 123- bus reactive load, the 123-bus system DERs reactive power generation and the bid/offer values of reactive power of 123- bus system ADS for β=1.

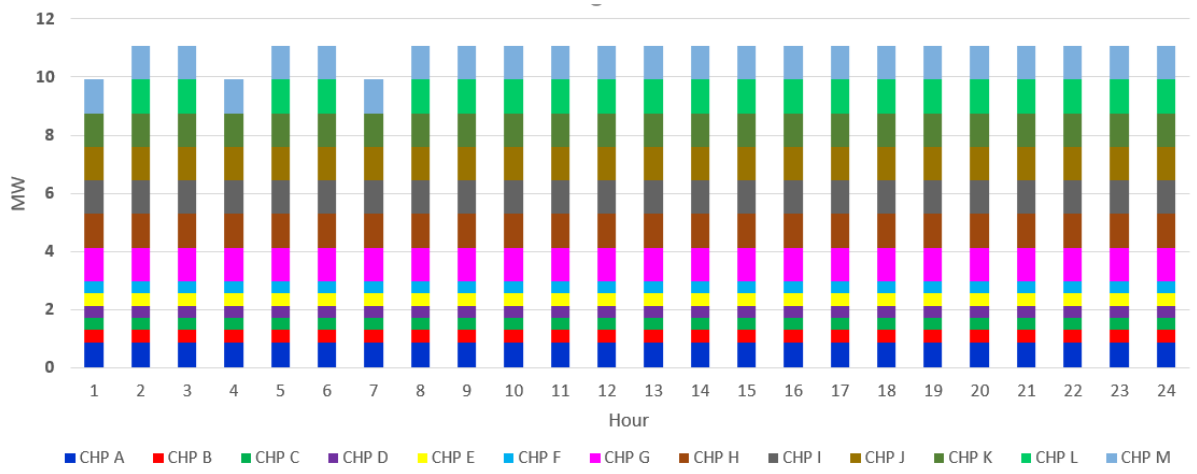

(a)

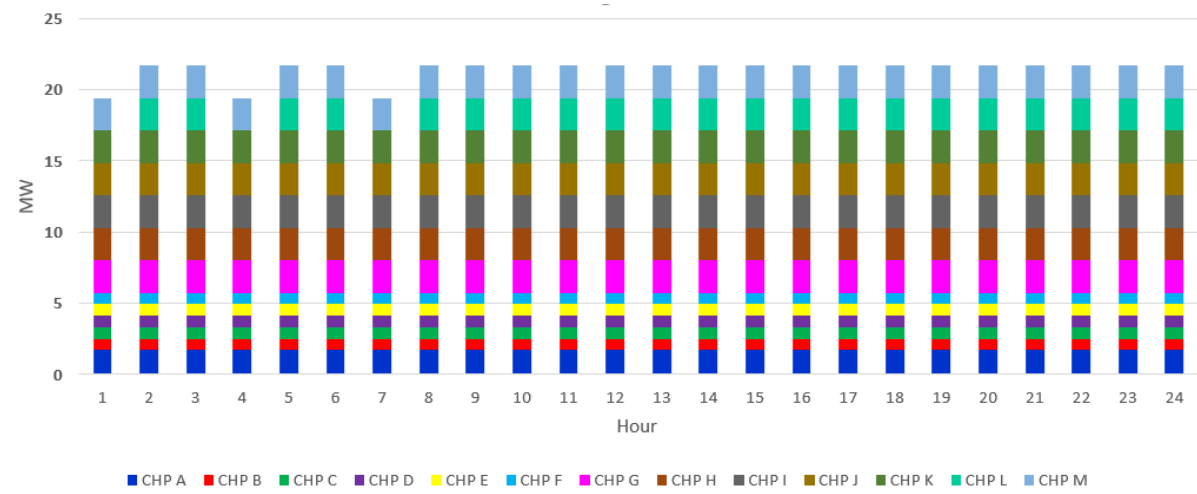

(b)

Fig. 19. (a) The CHPs electricity dispatch of the 123-bus system. (b) The CHPs heating dispatch of the 123-bus system for β=1.

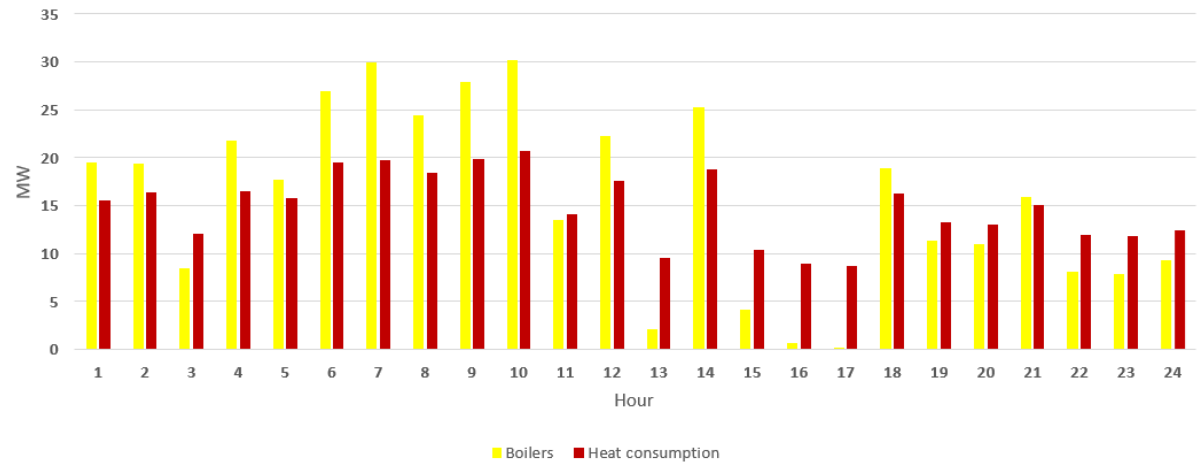

Fig. 20. The boilers heating dispatch of the 123-bus system for β=1.

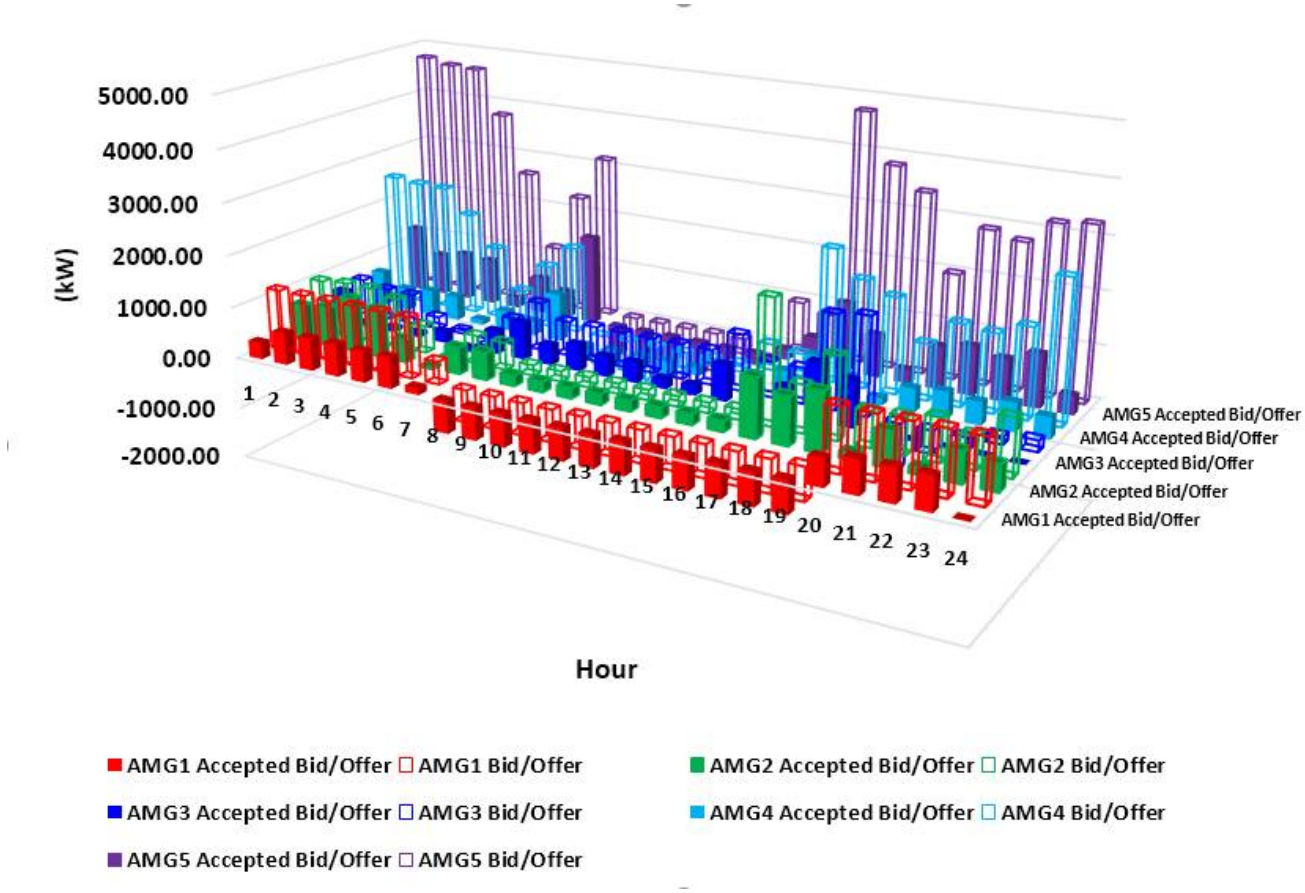

Fig. 21. The values of AMGs bids/offers and AMGs accepted bids/offers.

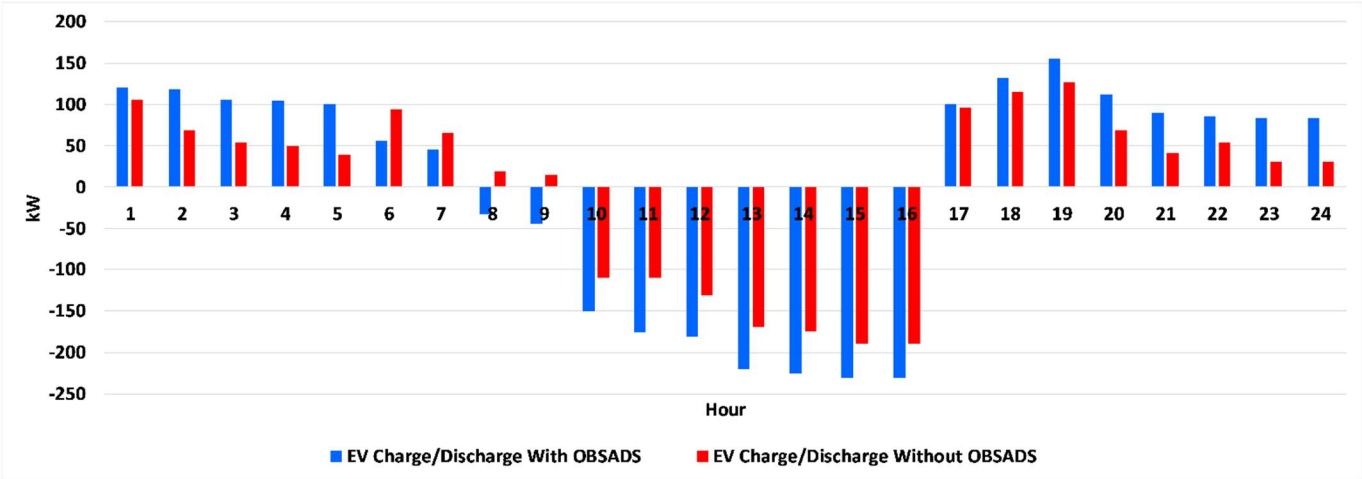

Fig. 22. The charge and discharge of PHEVs for OBSADS and without OBSADS cases.

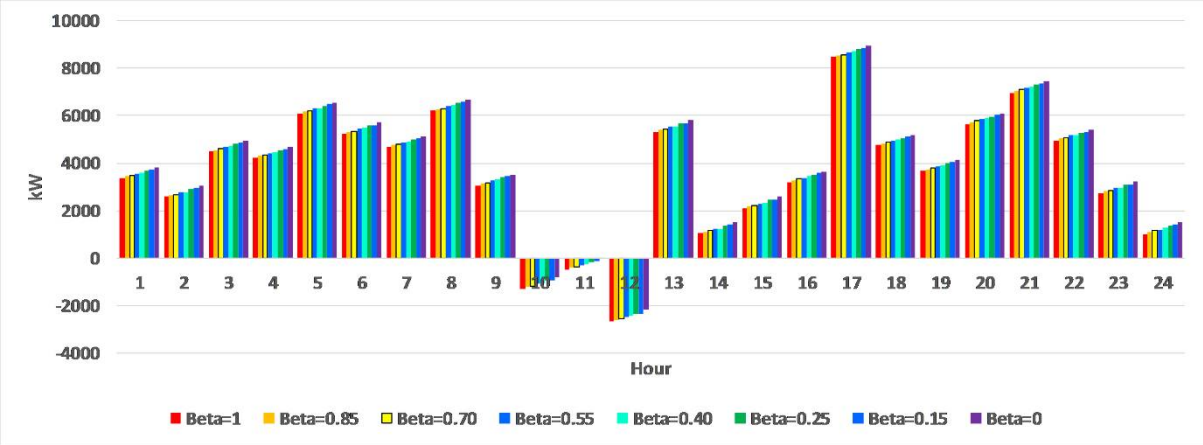

(a)

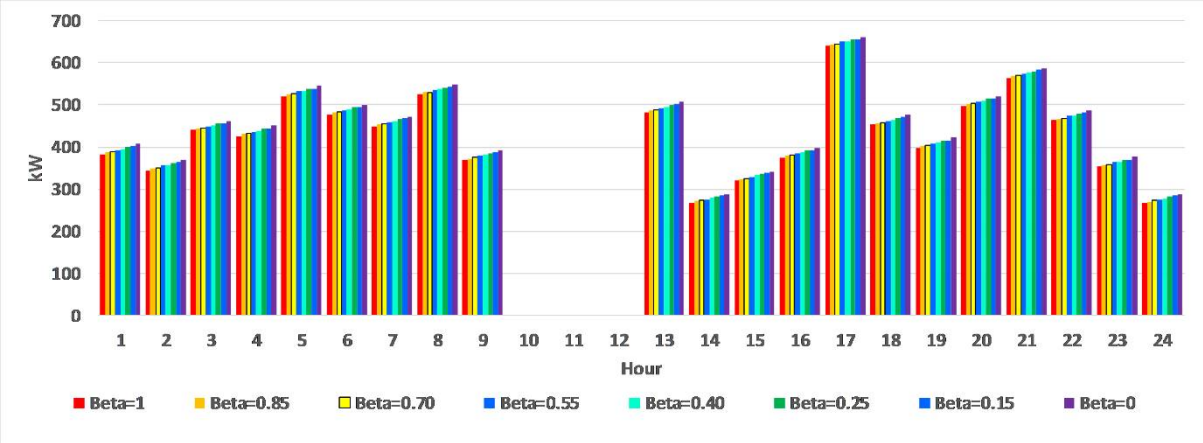

(b)

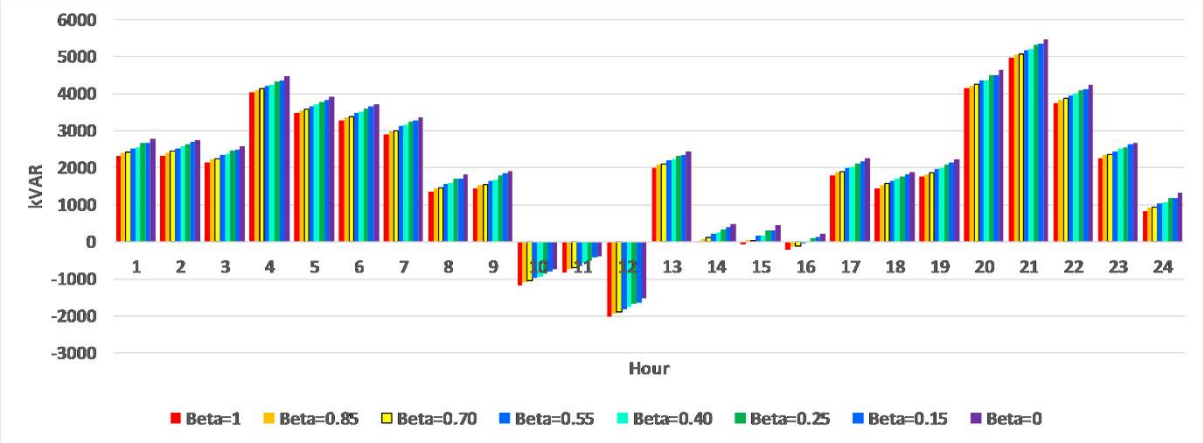

(c)

Fig. 23. The bid/offer values of (a) active power, (b) spinning reserve and, (c) reactive power of 123- bus system ADS for different values of β.

Table 2. The optimal switching device status for the normal and the zonal worst-case contingent conditions of the 123-bus test system.

State	Fault Number	SW1	SW2	SW3	SW4	SW5	SW6	SW7	SW8	SW9	SW10	SW11
Normal	----	1	0	1	1	1	0	0	0	0	0	0
Fault: L13-18 (Zone 1)	1	1	0	1	1	1	0	1	1	0	0	0
Fault: L13-34 (Zone 1)	2	1	0	1	1	1	0	0	0	1	0	0
Fault: L18-21 (Zone 1)	3	1	0	1	1	1	0	0	0	0	1	0
Fault: L25-28 (Zone 1)	4	1	0	1	1	1	0	0	0	0	0	1
Fault: L 8-13 (Zone 1)	5	0	0	1	1	1	1	0	1	1	0	0
Fault: L135-35 (Zone 2)	6	1	0	1	1	0	0	0	0	0	0	0
Fault: L49-50 (Zone 2)	7	1	0	1	1	1	1	0	0	0	0	0
Fault: L40-42 (Zone 2)	8	1	0	1	1	1	1	0	0	0	0	0
Fault: L51-151 (Zone 2)	9	1	0	1	1	1	1	0	0	0	1	0
Fault: L36-38 (Zone 2)	10	1	0	1	1	1	0	1	0	0	0	0
Fault: L54-57 (Zone 3)	11	1	1	1	1	1	0	0	0	0	0	0
Fault: L60-62 (Zone 3)	12	1	0	1	1	1	0	1	1	0	0	0
Fault: L57-60 (Zone 3)	13	1	1	1	1	1	0	0	0	1	0	0
Fault: L63-64 (Zone 3)	14	1	0	1	1	1	0	0	1	0	0	0
Fault: L152-52 (Zone 3)	15	0	1	1	1	1	0	0	0	0	0	0
Fault: L101-105 (Zone 4)	16	1	0	1	1	1	1	0	0	0	0	0
Fault: L105-108 (Zone 4)	17	1	0	1	1	1	1	0	0	0	0	0
Fault: L101-97 (Zone 4)	18	1	0	1	1	1	1	0	0	1	0	0
Fault: L101-102 (Zone 4)	19	1	0	1	1	1	0	0	0	0	0	0
Fault: L109-110 (Zone 4)	20	1	0	1	1	1	0	0	0	0	0	0
Fault: L72-76 (Zone 5)	21	1	1	1	1	1	0	0	0	0	0	0
Fault: L86-87 (Zone 5)	22	1	1	1	1	1	0	0	0	0	0	0
Fault: L72-67 (Zone 5)	23	1	1	1	1	1	0	0	0	0	0	0
Fault: L80-81 (Zone 5)	24	1	0	1	1	1	0	0	0	0	0	0
Fault: L93-91 (Zone 5)	25	1	1	1	1	1	0	0	0	0	0	0

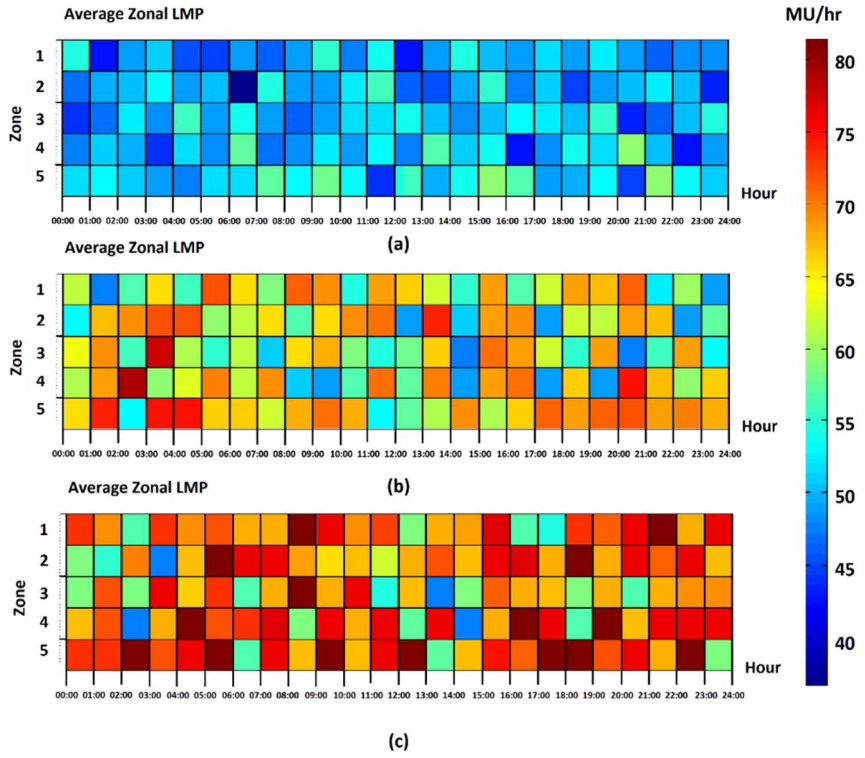

Fig.24. the estimated hourly average zonal LMP values for (a) normal condition, (b) Fault:L60-62 (Zone 3), and (c) Fault: L13-18 (Zone 1) contingent conditions for β=1.

Fig.25 shows the values of AMGs bids/offers and AMGs accepted bids/offers for the RT market. The maximum and minimum value of the AMGs bid/offer are 397.791 (kW) and -388.86 (kW) that belong to the AMG1 for 08:00 PM and 01:00 PM, respectively. The maximum and minimum value of the accepted AMGs bid/offer are 127.465 (kW) and -315.522 (kW) that belong to the AMG3 for 07:00 AM and 03:00 PM, respectively. Fig. 26 shows the estimated 15 minutes average zonal LMP values for (a) normal condition, (b) Fault: L60-62 (Zone 3), and (c) Fault: L13-18 (Zone 1) contingent conditions of the 123-bus test system. The range of estimated values of zonal LMP is increased for contingent conditions.

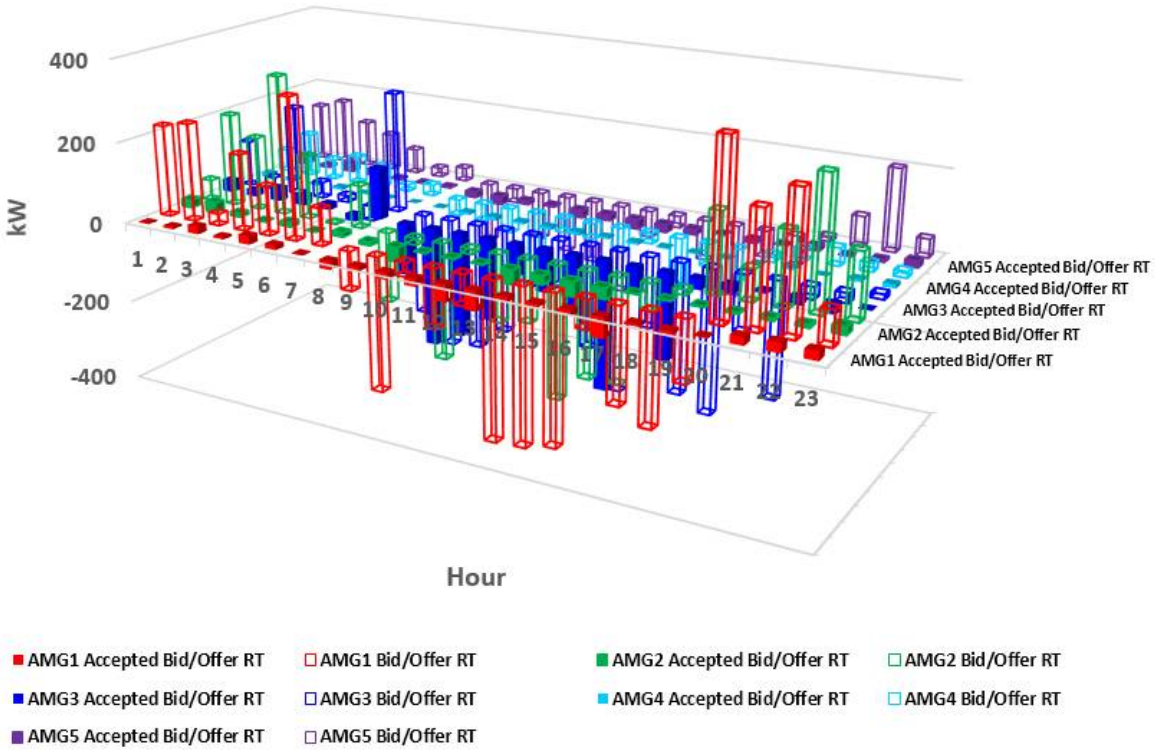

Fig.25. The values of AMGs bids/offers and AMGs accepted bids/offers for the RT market.

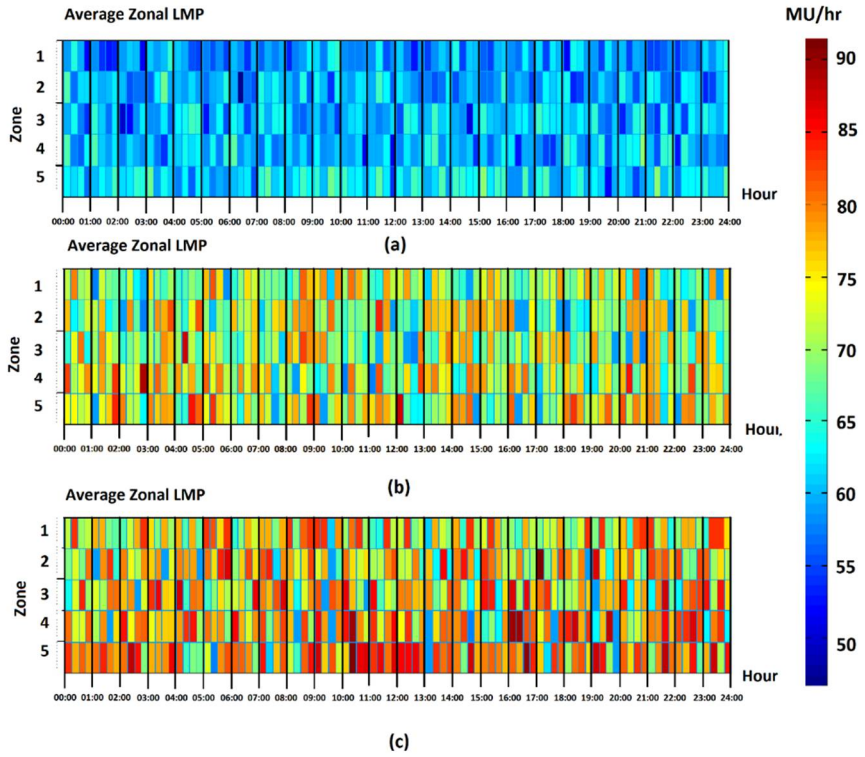

Fig. 26. shows the estimated 15 minutes average zonal LMP values for (a) normal condition, (b) Fault: L60-62 (Zone 3), and (c) Fault: L13-18 (Zone 1) contingent conditions of the 123-bus test system for β=1.

Fig. 27 depicts the bid/offer values of (a) active power, (b) spinning reserve and, (c) reactive power of 123- bus system ADS for different values of β, respectively. As shown in Fig. 27, as the value of β is increased, the absolute values of ADS bids/offers are decreased based on the fact that the ADSO chooses a risk-averse bidding strategy. Fig. 28 depicts the expected benefit/cost of 123- bus system ADS for bid/offer values of (a) DA markets of active power, spinning reserve and reactive power, (b) RT markets of active power and reactive power for different values of β. The uncertainty of parameters in the RT market has changed the forecasted values of DA parameters. Thus, when the value of β increases, the expected benefit of ADS does not decrease in some hours based on the fact that the difference of the DA forecasted and RT values of parameters are higher than the acceptable mismatch of the DA forecasting algorithm.

Table 3 presents the values of *ADZLMP* for the DA market of the first and second case studies and for their worst-case contingency and normal states. As shown in Table 3, the OBSADS procedure decreased the average of *ADZLMP* about 26.44% and 15.81% for the normal and worst-case contingency, respectively. The maximum difference between *ADZLMP* of the first and second cases takes on a value 0.1653 that is for the worst-case contingent conditions of the third zone.

Three Sensitivity Analysis (SA) was performed for analysing the impact of the change of energy and ancillary services prices on the ADS costs/benefits. Table 4 depicts the characteristics of the SA. The DA and RT energy and ancillary services prices have correlations and a single parameter sensitivity analysis cannot be performed.

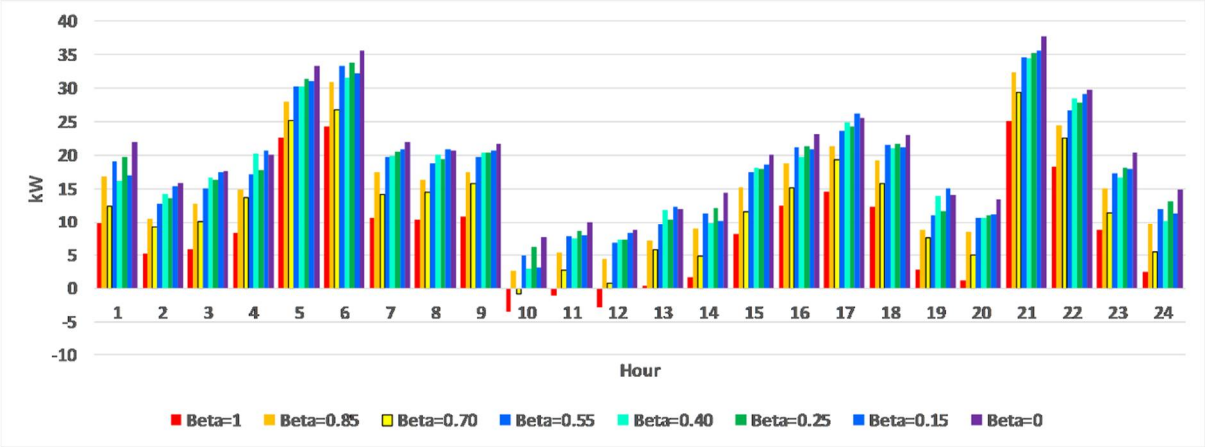

(a)

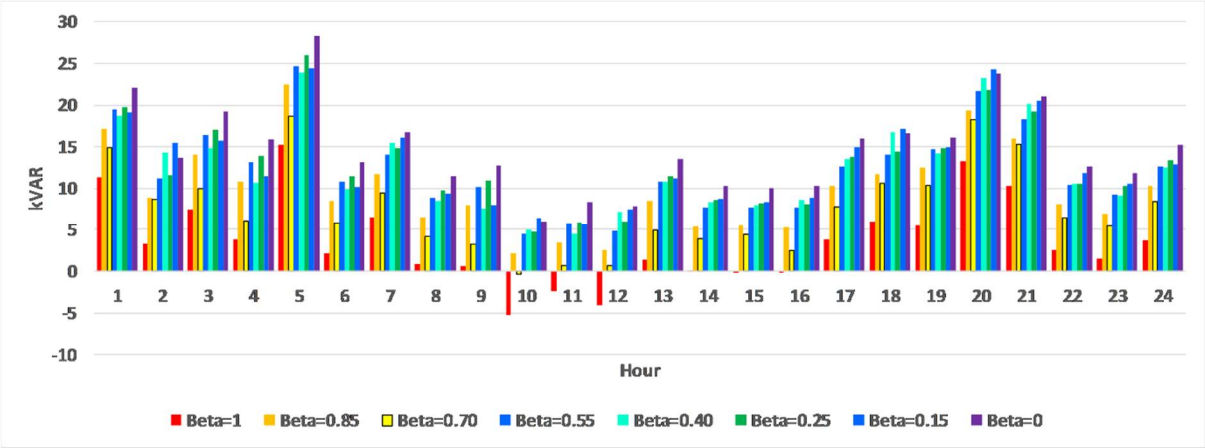

(c)

Fig. 27. The bid/offer values of (a) active power, (b) reactive power of 123- bus system ADS for different values of β in the RT market.

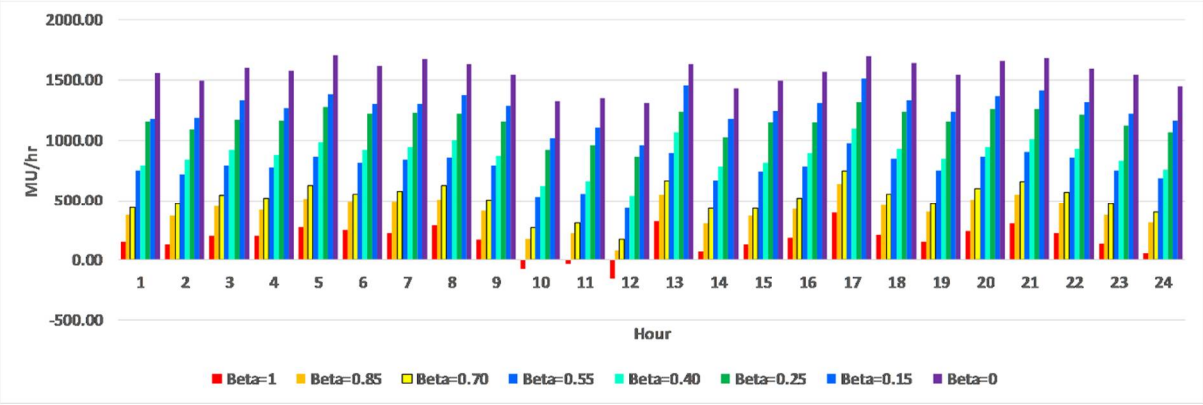

(a)

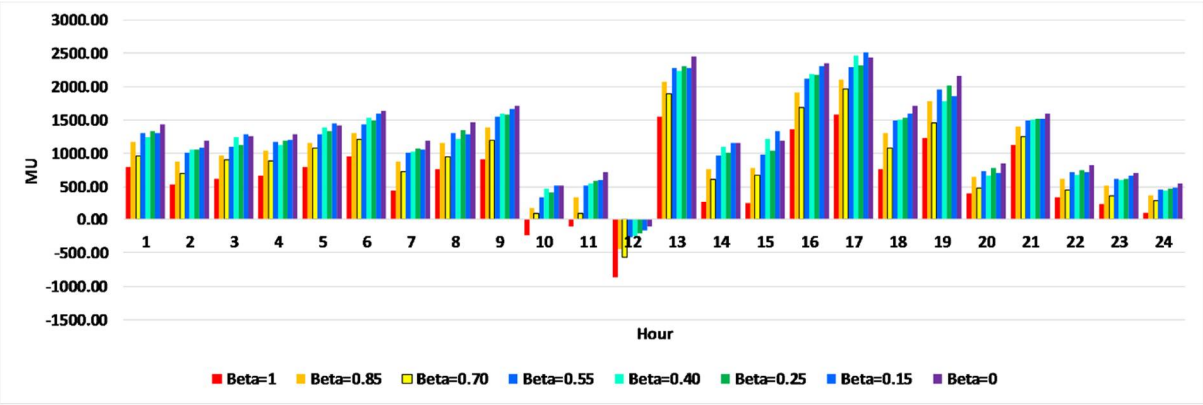

(b)

Fig. 28. The expected benefit/cost of 123- bus system ADS for bid/offer values of (a) DA markets of active power, spinning reserve and reactive power, (b) RT markets of active power and reactive power (15 minutes interval) for different values of β.

Table 3. The values of *ADZLMP* for the DA market of the first and second case studies and for their worst-case contingency and normal states.

Zone	*ADZLMP* normal state (first case)	*ADZLMP* worst-case zonal contingency (first case)	*ADZLMP* normal state (second case)	*ADZLMP* worst-case zonal contingency (second case)
1	0.8326	0.9516	0.6124	0.8012
2	0.7906	0.9607	0.6325	0.8226
3	0.8512	0.9782	0.6921	0.8129
4	0.8709	0.9421	0.7215	0.7915
5	0.8147	0.9511	0.6363	0.7964
Average	0.8326	0.9516	0.6124	0.8012

Table 4. The characteristics of parameters change in the sensitivity analysis

Case	Percent of DA energy price increased/decreased	Percent of day-ahead SR price increased/decreased	Percent of DA reactive power price increased/decreased	Percent of RT energy price increased/decreased	Percent of RT reactive power price increased/decreased
Base	--	--	--	--	--
SA1	-3%	-3%	-3%	-3%	-3%
SA2	+3%	+3%	+3%	+3%	+3%
SA3	-5%	-5%	-5%	-5%	-5%

Fig.29 (a) and (b) show the ADS revenue for DA energy and ancillary service markets for different SA conditions. The maximum decrease of DA energy, SR and reactive markets revenue values for the SA1 are 2.992%, 2.995% and 2.998%, respectively that are corresponding to the β=0.7, β=0.85, and β=0.25. The maximum increase of DA energy, SR and reactive markets revenue values for the SA2 are 3.021%, 3.172% and 3.033%, respectively that are corresponding to the β=1, β=0.15, and β=0.55. Finally, the maximum decrease of DA energy, SR and reactive markets revenue values for the SA3 are 4.998%, 4.976% and 4.997%, respectively that are corresponding to the β=0.55, β=0.25, and β=0.4.

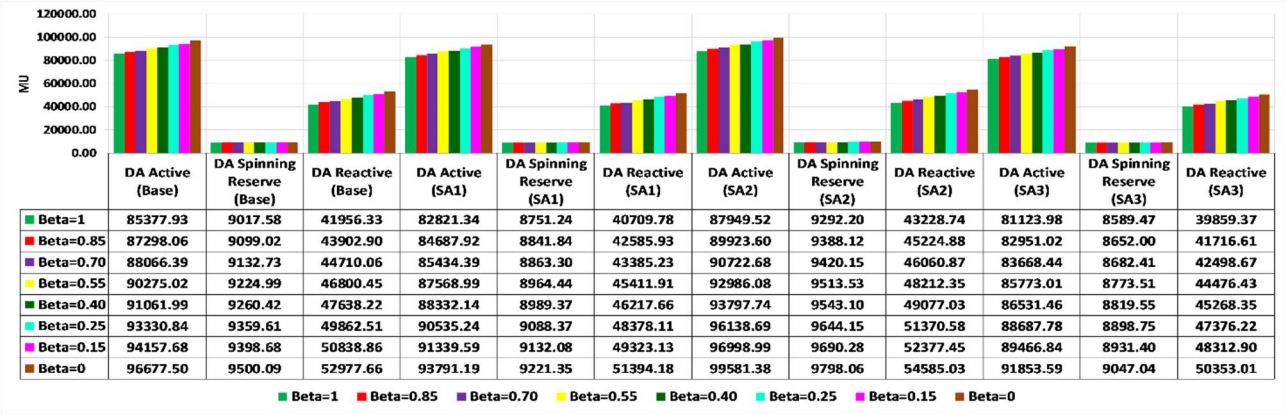

	DA Active (Base)	DA Spinning Reserve (Base)	DA Reactive (Base)	DA Active (SA1)	DA Spinning Reserve (SA1)	DA Reactive (SA1)	DA Active (SA2)	DA Spinning Reserve (SA2)	DA Reactive (SA2)	DA Active (SA3)	DA Spinning Reserve (SA3)	DA Reactive (SA3)
Beta=1	85377.93	9017.58	41956.33	82821.34	8751.24	40709.78	87949.52	9292.20	43228.74	81123.98	8589.47	39859.37
Beta=0.85	87298.06	9099.02	43902.90	84687.92	8841.84	42585.93	89923.60	9388.12	45224.88	82951.02	8652.00	41716.61
Beta=0.70	88066.39	9132.73	44710.06	85434.39	8863.30	43385.23	90722.68	9420.15	46060.87	83668.44	8682.41	42498.67
Beta=0.55	90275.02	9224.99	46800.45	87568.99	8964.44	45411.91	92986.08	9513.53	48212.35	85773.01	8773.51	44476.43
Beta=0.40	91061.99	9260.42	47638.22	88332.14	8989.37	46217.66	93797.74	9543.10	49077.03	86531.46	8819.55	45268.35
Beta=0.25	93330.84	9359.61	49862.51	90535.24	9088.37	48378.11	96138.69	9644.15	51370.58	88687.78	8898.75	47376.22
Beta=0.15	94157.68	9398.68	50838.86	91339.59	9132.08	49323.13	96998.99	9690.28	52377.45	89466.84	8931.40	48312.90
Beta=0	96677.50	9500.09	52977.66	93791.19	9221.35	51394.18	99581.38	9798.06	54585.03	91853.59	9047.04	50353.01

(a)

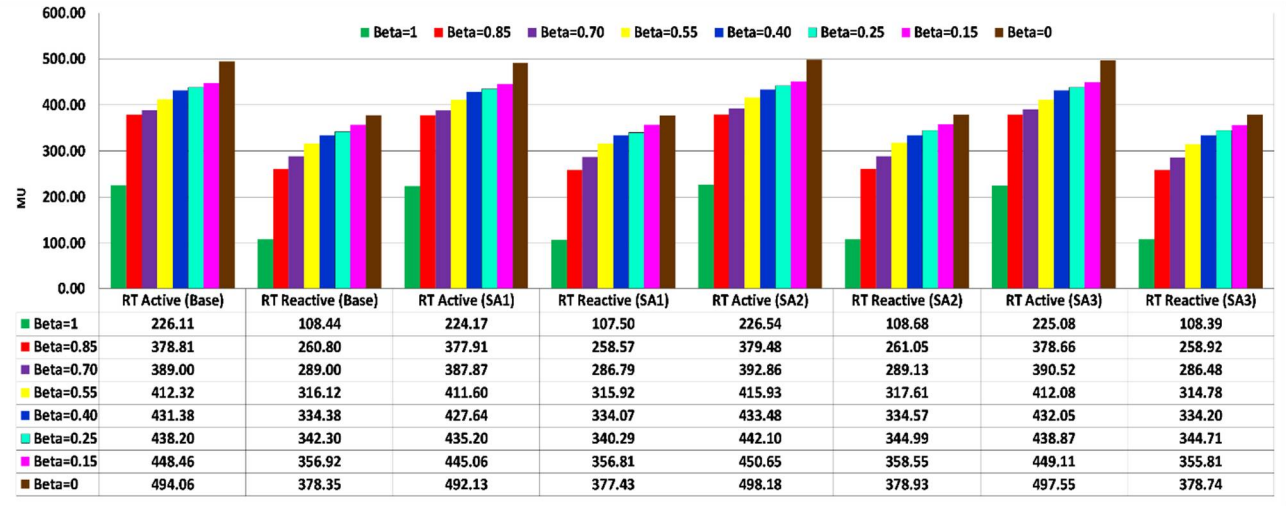

	RT Active (Base)	RT Reactive (Base)	RT Active (SA1)	RT Reactive (SA1)	RT Active (SA2)	RT Reactive (SA2)	RT Active (SA3)	RT Reactive (SA3)
Beta=1	226.11	108.44	224.17	107.50	226.54	108.68	225.08	108.39
Beta=0.85	378.81	260.80	377.91	258.57	379.48	261.05	378.66	258.92
Beta=0.70	389.00	289.00	387.87	286.79	392.86	289.13	390.52	286.48
Beta=0.55	412.32	316.12	411.60	315.92	415.93	317.61	412.08	314.78
Beta=0.40	431.38	334.38	427.64	334.07	433.48	334.57	432.05	334.20
Beta=0.25	438.20	342.30	435.20	340.29	442.10	344.99	438.87	344.71
Beta=0.15	448.46	356.92	445.06	356.81	450.65	358.55	449.11	355.81
Beta=0	494.06	378.35	492.13	377.43	498.18	378.93	497.55	378.74

(b)

Fig.29. (a) The ADS revenue for DA energy, (b) The ADS revenue for DA ancillary service markets for different SA conditions.

Fig. 30 depicts the aggregated daily ADS revenue for different values of β and sensitivity analysis conditions. The maximum percent of revenue changes of ADS is 324%, 318%, 331% and 313% for the base, SA1, SA2 and SA3 conditions and β=0, respectively. The minimum percent of revenue changes of ADS is 292%, 287%, 298% and 283% for the base, SA1, SA2 and SA3 conditions and β=1, respectively. Thus, the proposed OBSADS increased the ADS revenue for both risk-neutral and risk-averse bidding strategy of ADSO.

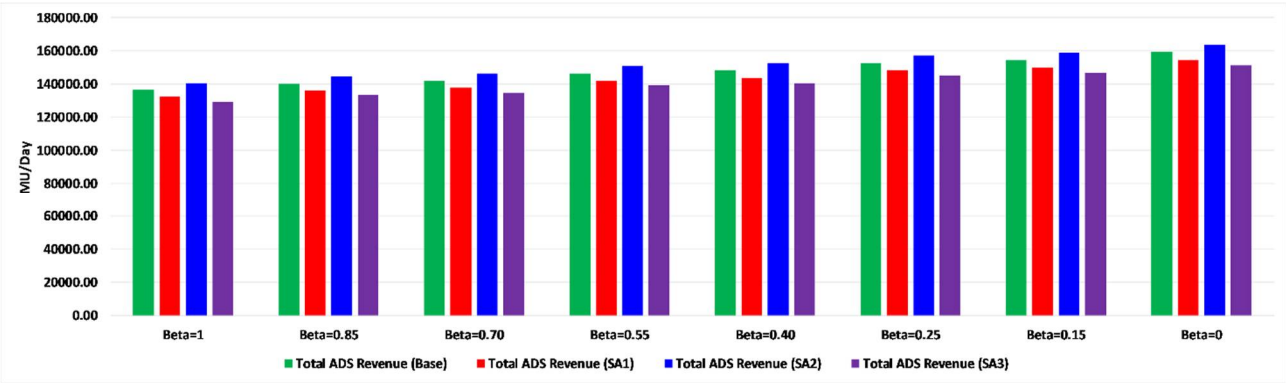

Fig. 30. The aggregated daily ADS revenue for different values of β and sensitivity analysis conditions

5. Conclusion

This paper addressed an integrated framework for optimal bidding strategy of ADS that its energy resources were combined heat and power units, small wind turbines, photovoltaic systems, gas-fired distributed generation and boilers, and plug-in electric vehicles. The proposed algorithm utilized an MINLP model to maximize distribution system and microgrids revenue. The proposed six-level algorithm optimized energy resource coordination of distribution system in the normal and contingent operational conditions. Two different cases were evaluated by different operational paradigms. The first case only considered the first and second level of optimization algorithm without any DRP implementation. The second case considered the six-level optimization procedure that utilized DRP alternatives for the optimal coordination of system resources in contingent conditions. Further, three sensitivity analyses were performed to assess the impact of energy and ancillary service prices changes on the distribution system revenue. The maximum percent of revenue changes of the distribution system was 324%, 318%, 331% and 313% for the base, 1st, 2nd and 3rd sensitivity analysis cases and risk-neutral bidding strategy, respectively. Further, the minimum percent of revenue changes of revenue was 292%, 287%, 298% and 283% for the base, 1st, 2nd and 3rd sensitivity analysis cases and risk-averse bidding strategy, respectively. Thus, the proposed OBSADS increased the distribution system revenue for both risk-neutral and risk-averse bidding strategies. The adoption of the proposed OBSADS increases the distribution system and microgrids revenues and optimizes the system resource coordination for the contingency conditions.

Acknowledgment

J.P.S. Catalão acknowledges the support by FEDER funds through COMPETE 2020 and by Portuguese funds through FCT, under POCI-01-0145-FEDER-029803 (02/SAICT/2017).

References

1- Wei Gu, Zhi Wub, Rui Bo, Wei Liu, Gan Zhou, Wu Chen, Zaijun Wu, Modeling," Planning and optimal energy management of combined cooling, heating and power microgrid: A review", *Electr. Power Energy Syst.*, 2014, **54**, pp. 26–37.

2- S. Chowdhury, S.P. Chowdhury and P. Crossley, "Microgrids and active distribution networks", The institution of engineering and technology, 2009.

3- Aringhieri R, Malucelli F., "Optimal operations management and network planning of a district system with a combined heat and power plant". *Annals of Operations Research,* 2003,**120**, pp.173–199.

4- Chicco G, Mancarella P., "Distributed multi-generation: a comprehensive view", *Renew. Sustain. Energy Revs.*, 2009, **13**, pp. 535–551.

5- Ran Wang, Ping Wang, Gaoxi Xiao, "A robust optimization approach for energy generation scheduling in microgrids", *Energy Convers. Manage.*, 2015, **106**, pp. 597-607.

6- Abdorreza Rabiee, Mohammad Sadeghi, Jamshid Aghaei, Alireza Heidari, "Optimal operation of microgrids through simultaneous scheduling of electrical vehicles and responsive loads considering wind and PV units uncertainties", *Renew. Sustain. Energy Rev.,* 2016, **57**, pp. 721-739.

7- Zeyu Wang , Ahlmahz Negash, Daniel S. Kirschen, "Optimal scheduling of energy storage under forecast uncertainties", *IET Gener. Transm. Distrib*., 2017, **11**, pp. 4220-4226.

8- José Iria, Filipe Soares, Manuel Matos, "Optimal bidding strategy for an aggregator of prosumers in energy and secondary reserve markets", *Applied Energy,* 2019, **238,** pp. 1361-1372.

9- Nima Nikmehr, Sajad Najafi-Ravadanegh, Amin Khodaei, " Probabilistic optimal scheduling of networked microgrids considering time-based demand response programs under uncertainty", *Applied Energy,* 2017, **198,** pp. 267-279.

10- Alipour M, Mohammadi-Ivatloo B, Zare K., "Stochastic risk-constrained short-term scheduling of industrial cogeneration systems in the presence of demand response programs", *Applied Energy,* 2014, **136,** pp. 393-404.

11- Vahid Hosseinnezhad, Mansour Rafiee, Mohammad Ahmadian, Pierluigi Siano, "Optimal day-ahead operational planning of microgrids", *Energy Convers. Manage.*, 2016, **126**, pp. 142-157.

12- Jamshid Aghaei, Vassilios G. Agelidis, Mansour Charwand, Fatima Raeisi, Abdollah Ahmadi, Ali Esmaeel Nezhad, Alireza Heidari, "Optimal Robust Unit Commitment of CHP Plants in Electricity Markets Using Information Gap Decision Theory", *IEEE Trans. on Smart Grid,* 2017, **8** , pp. 2296-304.

13- Saemeh Aghajani, Mohsen Kalantar, "Operational scheduling of electric vehicles parking lot integrated with renewable generation based on bilevel programming approach", *Energy*, 2017, **39,** pp. 422-432.

14- Jianxiao Wang, Haiwang Zhong, Wenyuan Tang, Ram Rajagopal, Qing Xia, Chongqing Kang, Yi Wang, Optimal bidding strategy for microgrids in joint energy and ancillary service markets considering flexible ramping products", *Applied Energy,* 2017, **205,** pp. 294-303.
15- Mohammadreza Mazidi, Alireza Zakariazadeh, Shahram Jadid, Pierluigi Siano, "Integrated scheduling of renewable generation and demand response programs in a microgrid", *Energy Convers. Manage.,* 2014, **86**, pp. 1118-1127.
16- Alipour M, Mohammadi-Ivatloo B, Zare K.,"Stochastic scheduling of renewable and CHP- based microgrids". *IEEE Trans. on Industrial Informatics*. 2015, **11**, pp.1049-58.
17- 18Mohammad H. Shams, Majid Shahabi, Mohammad E. Khodayar, "Stochastic day-ahead scheduling of multiple energy carrier microgrids with demand response", *Energy,* 2018, **155** , pp. 326-338.
18- A. Zakariazadeh, S. Jadid, and P. Siano, "Smart microgrid energy and reserve scheduling with demand response using stochastic optimization," *Elect. Power and Energy Syst.,* 2014, **63**, pp. 523–533.
19- Mushfiqur R. Sarker , Hrvoje Pandžić, Kaiwen Sun, Miguel A. Ortega-Vazquez, "Optimal operation of aggregated electric vehicle charging stations coupled with energy storage", *IET Gener. Transm. Distrib*., 2018, **12**, pp. 1127-1136.
20- Bingying Zhang, Qiqiang Lia, Luhao Wang, Wei Feng," Robust optimization for energy transactions in multi-microgrids under uncertainty", *Applied Energy*, 2018, **217**, pp. 346–360.
21- Alireza Zakariazadeh, Shahram Jadid, Pierluigi Siano, "Multi-objective scheduling of electric vehicles in smart distribution system", *Energy Convers. Manage.*, 2014, **79**, pp. 43-53.
22- S. Muhammad Bagher Sadati, Jamal Moshtagh, Miadreza Shafie-khah, João P.S. Catalão, "Smart distribution system operational scheduling considering electric vehicle parking lot and demand response programs", *Electr. Power Syst. Res.*, 2018, **160**, pp. 404-418.
23- Farhad Samadi Gazijahani, Javad Salehi, "Integrated DR and reconfiguration scheduling for optimal operation of microgrids using Hong's point estimate method ", *Electr. Power Syst. Res.*, 2018, **99**, pp. 481-492.
24- Alireza Majzoobi, Amin Khodaei, "Application of microgrids in supporting distribution grid flexibility", *IEEE Trans. on Power Sys.,* 2017, **32**, pp. 3660-3669.
25- Abhishek Kumar, Nand K. Meena, Arvind R. Singh, et.al," Strategic integration of battery energy storage systems with the provision of distributed ancillary services in active distribution systems", *Applied Energy,* 2019, **253,** 113503.
26- M. Hemmati, B. Mohammadi-Ivatloo, S. Ghasemzadeh, E. Reihani, "Risk-based optimal scheduling of reconfigurable smart renewable energy based microgrids", *Int. J. Electr. Power Energy Syst*., 2018, **101**, pp. 415-428.
27- Yixin Liu, Li Guo, Chengshan Wang, "A robust operation-based scheduling optimization for smart distribution networks with multi-microgrids", *Applied Energy*, 2018, **228**, pp. 130-140.
28- Sajad Tabatabaee, Seyed Saeedallah Mortazavi, Taher Niknam, "Stochastic scheduling of local distribution systems considering high penetration of plug-in electric vehicles and renewable energy sources", *Energy,* 2018, **121** , pp. 480-490.
29- Vahid Davatgaran, Mohsen Saniei, Seyed Saeidollah Mortazavi, "Smart distribution system management considering electrical and thermal demand response of energy hubs", *Energy*, 2019, **169**, pp. 38-49.
30- Mousa Marzband, Masoumeh Javadi, S. Ali Pourmousavi, Gordon Lightbody, "An advanced retail electricity market for active distribution systems and home microgrid interoperability based on game theory", *Electr. Power Syst. Res.*, 2018, **157** , pp. 187-199.
31- Saeed Abapour, Behnam Mohammadi-Ivatloo, Mehrdad Tarafdar Hagh," Robust bidding strategy for demand response aggregators in electricity market based on game theory", ", *J. Cleaner Production,* 2020, **243**, 118393.
32- W. Hedman, M.Ferris, et al.: 'Co-Optimization of Generation Unit Commitment and Transmission Switching With N-1 Reliability', *IEEE Trans. on Power Sys.,* 2010, **25**, pp. 1052-1063.
33- Farid Varasteh, Mehrdad Setayesh Nazar, Alireza Heidari, Miadreza Shafie-khah, João P. S. Catalão, "Distributed energy resource and network expansion planning of a CCHP based active microgrid considering demand response programs", *Energy*, 2019, **172**, pp. 19-105.
34- R. Mehta, , D. Srinivasan, Jing Yang, "Double-layered intelligent energy management for optimal integration of plug-in electric vehicles into distribution systems", *Applied Energy,* 2019, **233-234**, pp. 145-155.
35- Mehrdad Setayesh Nazar, Ashkan Eslami Fard, Alireza Heidari, Miadreza Shafie-khah, João P.S. Catalão," Hybrid model using three-stage algorithm for simultaneous load and price forecasting", *Electr. Power Syst. Res.*, 2018, **165**, pp. 214-228.
36- Ben-Tal, A. and A. Nemirovski, "On polyhedral approximations of the second-order cone", *Mathematics of Operations Research*, 2001. **26**(2): pp. 193-205.
37- Gabriel Luque and Enrique Alba," Parallel Genetic Algorithms: Theory and Real World Applications", 2011, Springer-Verlag Berlin Heidelberg.
38- Wallace SW, Ziemba WT. Applications of stochastic programming. MPS-SIAM; 2005.
39- Baran, M.E., Wu, F.F.: 'Network reconfiguration in distribution systems for loss reduction and load balancing', IEEE Trans. Power. Del., 1989, 4, (2), pp. 1401-1407.